

# Irrigation quantification through backscatter data assimilation with a buddy check approach

Louise Busschaert<sup>1</sup>, Michel Bechtold<sup>1</sup>, Sara Modanesi<sup>2</sup>, Christian Massari<sup>3</sup>, Luca Brocca<sup>3</sup>, and Gabrielle J.M. De Lannoy<sup>4</sup>

<sup>1</sup>KU Leuven

<sup>2</sup>Research Institute for Geo-Hydrological Protection, National Research Council

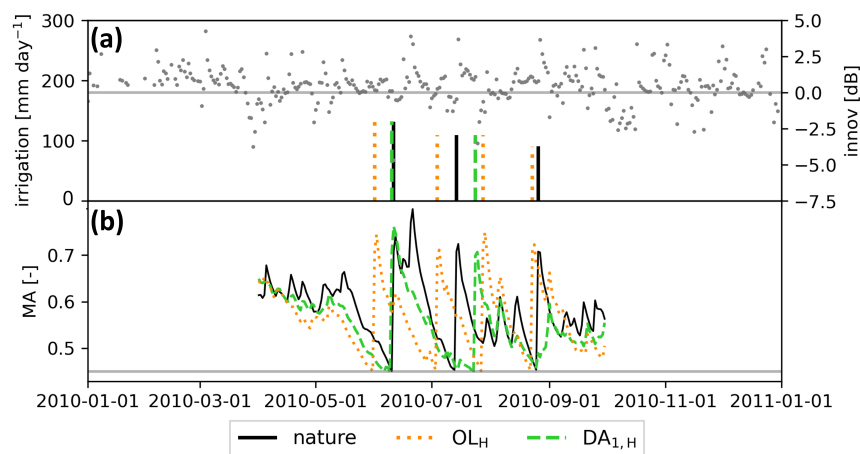
<sup>3</sup>National Research Council

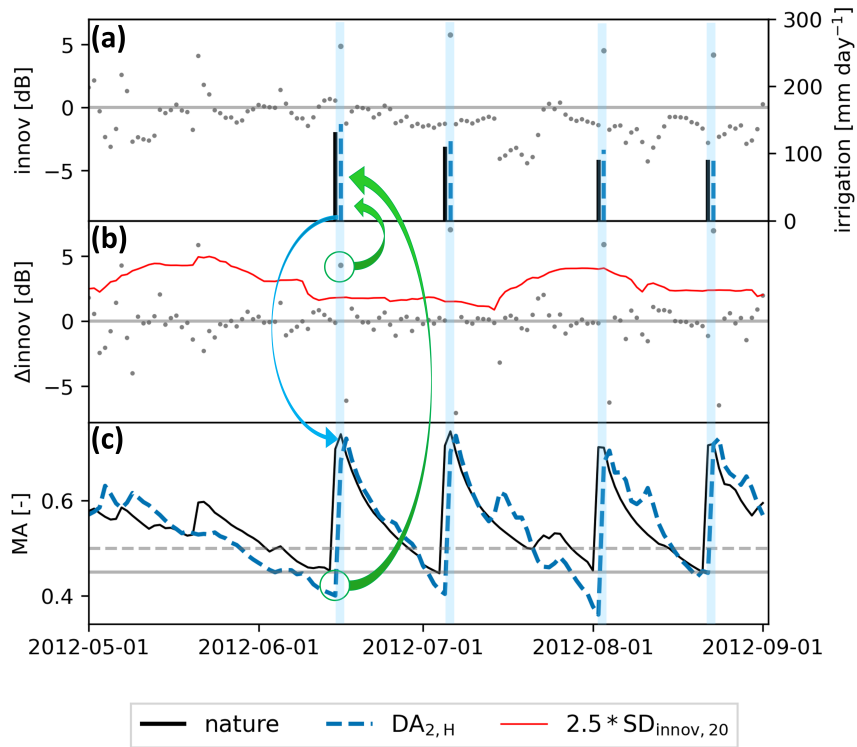
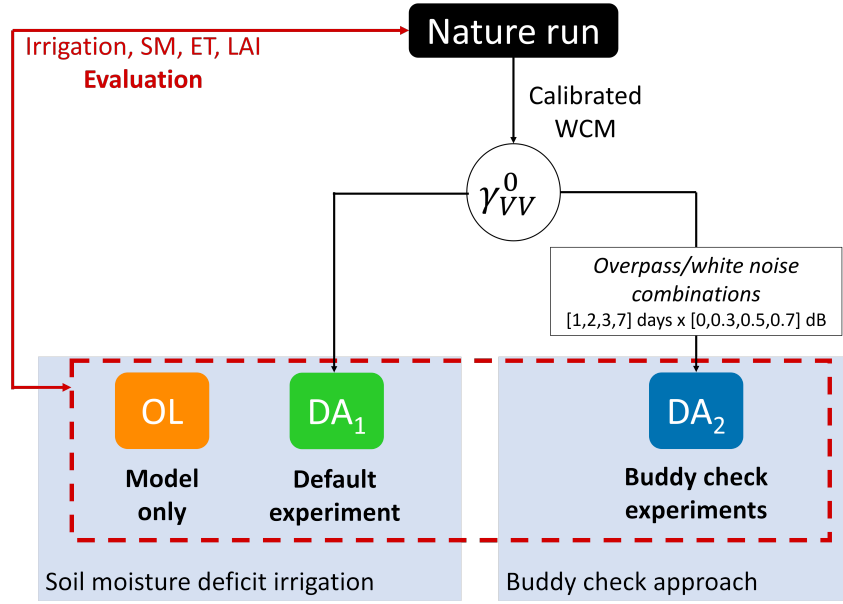
<sup>4</sup>KU Leuven, Department of Earth and Environmental Sciences

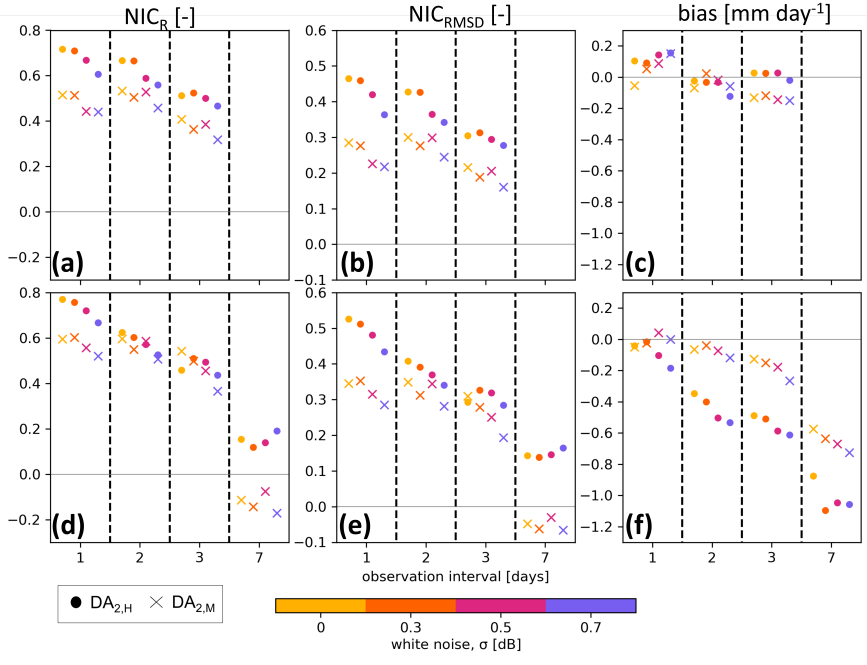
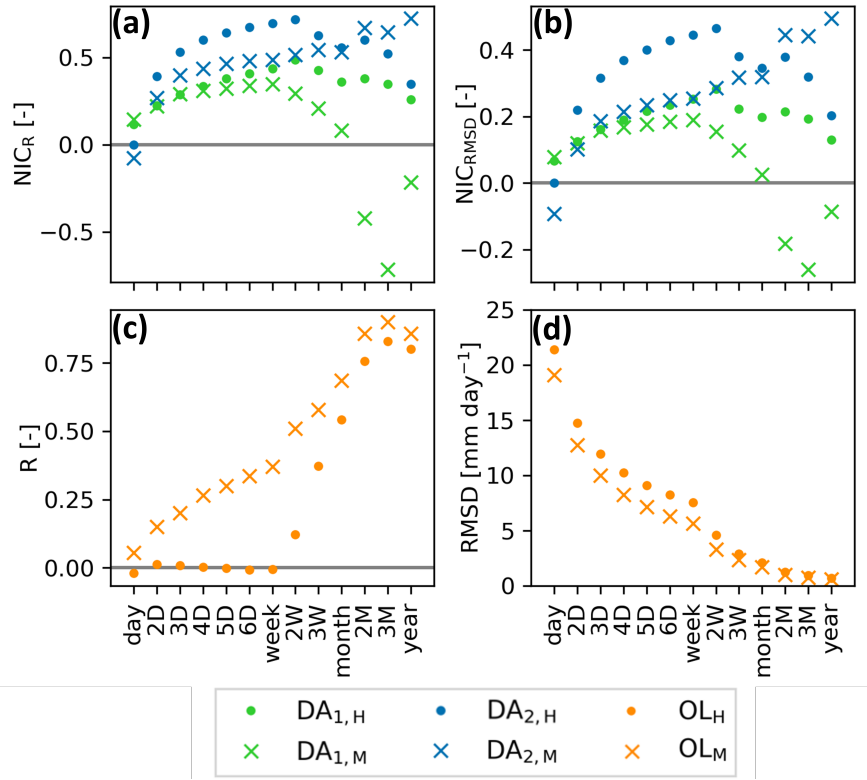
February 9, 2023

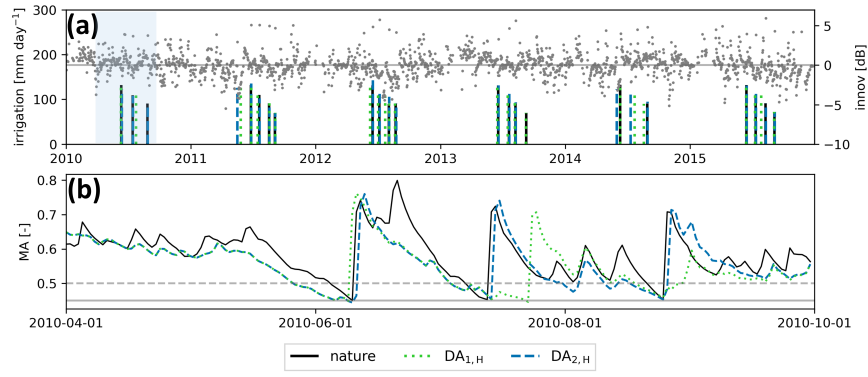
## Abstract

Irrigation is an important component of the terrestrial water cycle, but it is often poorly accounted for in models. Recent studies have attempted to integrate satellite data and land surface models via data assimilation (DA) to (1) detect and quantify irrigation, and (2) better model the related land surface variables such as soil moisture, vegetation, and evapotranspiration. In this study, different synthetic DA experiments are tested to advance satellite DA for the estimation of irrigation. We assimilate synthetic Sentinel-1 backscatter observations into the Noah-MP model coupled with an irrigation scheme. When updating soil moisture, we found that the DA sets better initial conditions to trigger irrigation in the model. However, large DA updates to wetter conditions can inhibit irrigation simulation. Building on this limitation, we propose an improved DA algorithm using a buddy check approach. The method still updates the land surface, but now the irrigation trigger is not based on the evolution of soil moisture, but on an adaptive innovation outlier detection. The new method was tested with different levels of model and observation error. For mild model and observation errors, the DA outperforms the model-only 14-day irrigation estimates by about 30% in terms of root-mean-squared differences, when frequent (daily or every other day) observations are available. The improvements can surpass 50% for high forcing errors. However, with longer observation intervals (7 days), the system strongly underestimates the irrigation amounts. The method is flexible and can be expanded to other DA systems and to a real world case.









1 **Irrigation quantification through backscatter data**  
2 **assimilation with a buddy check approach**

3 **L. Busschaert<sup>1</sup>, M. Bechtold<sup>1</sup>, S. Modanesi<sup>2</sup>, C. Massari<sup>2</sup>, L. Brocca<sup>2</sup>,**  
4 **G.J.M. De Lannoy<sup>1</sup>**

5 <sup>1</sup>Department of Earth and Environmental Sciences, KU Leuven, Heverlee, B-3001, Belgium

6 <sup>2</sup>Research Institute for Geo-hydrological Protection, National Research Council, Via della Madonna Alta  
7 126, 06128 Perugia, Italy

8 **Key Points:**

- 9 • Model-driven irrigation estimation has limitations, when solely based on improved  
10 soil moisture conditions obtained via data assimilation.  
11 • A new method based on an adaptive outlier detection improves the estimated irriga-  
12 tion in a synthetic data assimilation setup.  
13 • The method reduces irrigation errors by 30% for frequent assimilation of backscatter  
14 observations with reasonable levels of noise.

**Abstract**

Irrigation is an important component of the terrestrial water cycle, but it is often poorly accounted for in models. Recent studies have attempted to integrate satellite data and land surface models via data assimilation (DA) to (1) detect and quantify irrigation, and (2) better model the related land surface variables such as soil moisture, vegetation, and evapotranspiration.

In this study, different synthetic DA experiments are tested to advance satellite DA for the estimation of irrigation. We assimilate synthetic Sentinel-1 backscatter observations into the Noah-MP model coupled with an irrigation scheme. When updating soil moisture, we found that the DA sets better initial conditions to trigger irrigation in the model. However, large DA updates to wetter conditions can inhibit irrigation simulation. Building on this limitation, we propose an improved DA algorithm using a buddy check approach. The method still updates the land surface, but now the irrigation trigger is not based on the evolution of soil moisture, but on an adaptive innovation outlier detection.

The new method was tested with different levels of model and observation error. For mild model and observation errors, the DA outperforms the model-only 14-day irrigation estimates by about 30% in terms of root-mean-squared differences, when frequent (daily or every other day) observations are available. The improvements can surpass 50% for high forcing errors. However, with longer observation intervals (7 days), the system strongly underestimates the irrigation amounts. The method is flexible and can be expanded to other DA systems and to a real world case.

**Plain Language Summary**

Irrigation has an important impact on the terrestrial water cycle. However, it remains poorly simulated by models and it is hard to quantify through satellite observations alone. The combination of both models and satellite observations to detect and quantify irrigation has been explored in the last few years. Recently, Sentinel-1 radar (microwave) observations have been assimilated into the Noah-MP land surface model in order to quantify irrigation, and better estimate the related land surface variables, such as soil moisture and vegetation. This system has shown benefits but also limitations, which are highlighted and addressed in our study using synthetic experiments. We proposed an improved data assimilation algorithm and tested it for different levels of model and observation error. The new method estimates irrigation more accurately (30%) than the model alone, provided that frequent (daily or every other day) observations are available. With further developments, the new methodology could be used in a real-world experiment where it could ultimately contribute to the complex challenge of irrigation monitoring.

**1 Introduction**

Irrigation represents more than 70% of freshwater withdrawals (Gleick et al., 2009) making it the most important human activity impacting the terrestrial water cycle. Over the last decades, irrigated areas have expanded almost sixfold (Siebert et al., 2015), and contributed significantly to the increase in global crop production over the same time period (Foley et al., 2011). Under a growing population, food demand will continue to rise, which will inevitably lead to a further expansion and intensification of irrigated agriculture (Foley et al., 2011). In parallel, climate change will impact the irrigation water needs as a result of the expected rising temperatures and drier periods in many regions (Busschaert et al., 2022; Döll, 2002; Fischer et al., 2007). Conversely, irrigation also plays an important role in weather and climate dynamics (Bonfils & Lobell, 2007; Hirsch et al., 2017; Mahmood et al., 2014; Thiery et al., 2017, 2020), but it is still not or poorly included in Earth system models (Cook et al., 2015; Gormley-Gallagher et al., 2022; Valmassoi & Keller, 2022). Not only is there a call to monitor irrigation in order to ensure that the available water meets the

64 future irrigation demands, but future climate-related research, and Earth system models in  
65 general, could significantly benefit from large-scale irrigation estimates.

66 In the last years, several methods have been developed to map and quantify irrigation  
67 by making use of satellite remote sensing data (Massari et al., 2021). These observations  
68 (optical, microwave and gravimetric measurements) are used alone, combined with each  
69 other, or with models. Optical observations were first used to map irrigation relying on  
70 the difference in spectral responses between irrigated and non-irrigated areas (e.g., Ozdogan  
71 & Gutman, 2008; Pervez et al., 2014; Salmon et al., 2015; Xie & Lark, 2021; L. Zhang  
72 et al., 2022), and more recently machine learning-based methods have also been suggested  
73 (e.g., Jin et al., 2016; Magidi et al., 2021; Nagaraj et al., 2021; C. Zhang et al., 2022).  
74 Optical data have further been used to quantify irrigation amounts, mostly using estimates  
75 of actual evapotranspiration (ET) based on vegetation indices, sometimes also including  
76 models (land surface, water and energy balance), or other remote sensing data (e.g., thermal  
77 (e.g., Brombacher et al., 2022; Bretreger et al., 2022; Droogers et al., 2010; Le Page et al.,  
78 2012; Maselli et al., 2020; Olivera-Guerra et al., 2020; van Eekelen et al., 2015; Vogels et  
79 al., 2020). More recently optical leaf area index (LAI) observations have been assimilated  
80 into the Noah-MP land surface model (LSM; Niu et al., 2011) with a focus on improving  
81 irrigation estimations by updating the land surface (Nie et al., 2022).

82 While optical-based methods have progressed and shown some promising results, they  
83 typically rely on proxies, and are limited by cloud cover. By contrast, microwave signals  
84 can directly be related to water, and are not limited by atmospheric conditions. Despite  
85 their coarse resolutions, soil moisture retrievals from passive L-band radiometers or from  
86 active C-band scatterometers can detect wetter moisture when large-scale irrigation water  
87 is applied. The first microwave-based irrigation estimates were derived by inverting the soil  
88 water balance (SM2RAIN algorithm; Brocca et al., 2014) using several surface soil mois-  
89 ture (SSM) products (Soil Moisture Active Passive [SMAP], Soil Moisture Ocean Salinity  
90 [SMOS], Advanced SCATterometer [ASCAT], Advanced Microwave Scanning Radiometer  
91 2 [AMSR2]) at a 25-km resolution (Brocca et al., 2018). They found satisfactory results in  
92 terms of irrigation quantification, but the outcome strongly depended on the revisit and the  
93 uncertainty of the SSM retrievals. Following the same approach, Dari et al. (2020) achieved  
94 finer resolution quantification by downscaling SMAP and SMOS data using the Disaggre-  
95 gation based on Physical and Theoretical scale Change algorithm (DisPATCH; Merlin et  
96 al., 2008). Jalilvand et al. (2019) applied this method in a more arid climate (Iran). SSM  
97 retrievals (containing irrigation in the signal) were also contrasted against LSM simulations  
98 (without irrigation), in order to estimate the amounts of water applied (Zaussinger et al.,  
99 2019; Zohaib & Choi, 2020). Despite these methodological advances towards irrigation es-  
100 timation, the currently most accurate microwave-based satellite SSM retrievals are, for the  
101 time being, only available at resolutions coarser than most irrigated fields in Europe.

102 C-band synthetic aperture radar (CSAR) observations provide data at finer (field scale)  
103 resolutions, and they are also sensitive to soil moisture, albeit with less penetration depth  
104 than L-band observations. The Sentinel-1 (S1; Torres et al., 2012) mission from the Euro-  
105 pean Space Agency (ESA) offers the opportunity for frequent ( $\sim 2$ -3 day revisit in Europe)  
106 and fine-scale (10 m) observations, which are required for irrigation detection and quanti-  
107 fication purposes. The S1 mission comprises a constellation of two satellites (S1-A and S1-B)  
108 sensing in two polarizations over land: co-polarized VV (vertically transmitted, vertically re-  
109 ceived), and cross-polarized VH (vertically transmitted, horizontally received). In December  
110 2021, S1-B has become unresponsive, resulting in fewer observations from that time onwards.  
111 High-resolution SSM estimates retrieved from S1 backscatter have been developed in the last  
112 years. Zappa et al. (2021) used the TU Wien S1 SSM product (Bauer-Marschallinger et al.,  
113 2019) to detect and quantify irrigation at a local scale, based on spatiotemporal variations in  
114 SSM. The method showed promising results in terms of detection and correlation, but sys-  
115 tematic underestimations of the irrigation water amounts were found when the observation  
116 interval was longer than 1 day (in a follow-up synthetic experiment; Zappa et al., 2022). The

117 first regional datasets of high resolution irrigation water use, based on S1 data, have been  
 118 released by (Dari et al., in review) using the soil moisture-based inversion approach. While  
 119 the backscatter itself has already been used in irrigation mapping and timing studies at the  
 120 local scale (Bazzi, Baghdadi, Fayad, Zribi, et al., 2020; Bazzi, Baghdadi, Fayad, Charron, et  
 121 al., 2020), the direct use of S1 data to quantify irrigation is only in its infancy, as changes  
 122 in backscatter are affected by the water in the topsoil, but also by the vegetation (water,  
 123 volume, density, and geometry), and terrain roughness (McNairn & Shang, 2016).

124 The most optimal and spatio-temporally complete estimates of irrigation could theoret-  
 125 ically be expected to result from a combination of observations (e.g. microwave observations)  
 126 with models through data assimilation (DA; De Lannoy et al., 2022). Abolafia-Rosenzweig  
 127 et al. (2019) performed SMAP SSM DA into the variable infiltration capacity (VIC) LSM,  
 128 using a particle batch smoother. With the intent of going to a finer resolution, Das et al.  
 129 (in review) used a similar approach using the S1-SMAP SSM product (Das et al., 2019).  
 130 Ouaadi et al. (2021) assimilated S1-derived SSM data into the FAO-56 (Allen et al., 1998)  
 131 model with a particle filter. In the three aforementioned studies, a series of DA synthetic  
 132 experiments were carried out to evaluate the impact of e.g., time interval between the assim-  
 133 ilated observations and their level of error. They concluded that the proposed techniques  
 134 could accurately estimate irrigation amounts and timing (only for Ouaadi et al., 2021) but  
 135 that small errors (levels of noise) and frequent observations are crucial.

136 The above studies assimilated SSM products, but retrievals can introduce errors and  
 137 inconsistencies in the DA system (De Lannoy et al., 2022). Indeed, microwave-based re-  
 138 trievals often rely on ancillary data, and on empirical change detection algorithms in the  
 139 case of active measurements. Moreover, retrievals typically need rescaling to remove the  
 140 bias between the forecast (modeled) and observed soil moisture to achieve an optimal DA  
 141 system. These rescaling approaches sometimes remove irrigation from the signal (Kwon et  
 142 al., 2022). Based on these limitations, Modanesi et al. (2022) decided to directly assimilate  
 143 the S1 backscatter signal into the Noah-MP LSM (Niu et al., 2011) equipped with a sprin-  
 144 kler irrigation scheme (Ozdogan et al., 2010), where irrigation is dynamically modeled and  
 145 triggered based on a soil moisture deficit approach. The DA updated SSM and LAI using  
 146 an Ensemble Kalman Filter (EnKF) and a calibrated Water Cloud Model (WCM; Attema  
 147 & Ulaby, 1978; Modanesi et al., 2021) as observation operator to map between SSM, LAI  
 148 and backscatter. The idea is to provide the model with a better initial state, in terms of  
 149 soil moisture and vegetation, to improve the triggering and estimation of irrigation. How-  
 150 ever, the method has also shown several limitations related to the model (soil texture, crop  
 151 type, irrigation parametrization), and the DA system itself. An important problem is that  
 152 irrigation events could be missed when the DA updates soil moisture to wetter conditions  
 153 and thereby preventing irrigation simulation.

154 We set up synthetic experiments based on the system of Modanesi et al. (2022) with the  
 155 goal to investigate the exact benefits and shortcomings of S1 backscatter DA and to improve  
 156 the DA system with irrigation modeling (Section 2). In this context, synthetic backscatter  
 157 observations are generated from a nature run (also called ‘truth’) with a calibrated WCM  
 158 as observation operator (Modanesi et al., 2021). These observations are then assimilated  
 159 into model simulations, for which the forcings are altered compared to the reference nature  
 160 run. We then propose and test a novel method based on a buddy check approach. The  
 161 land surface state is still updated to have better initial conditions to estimate irrigation, but  
 162 the DA system now includes an adaptive innovation (observation *minus* forecast) outlier  
 163 detection. Anomalous high backscatter observations are not assimilated but used to flag  
 164 an unmodeled process and trigger irrigation when the conditions required for irrigation are  
 165 met, i.e., dry soil moisture and growing season. This new method is evaluated for different  
 166 forcing errors, observation intervals and observation errors in Section 3. Finally, we discuss  
 167 (Section 4) the possible future developments of the method, along with the opportunity to  
 168 bring this system to a real world experiment.

## 2 Data and Methods

### 2.1 Land surface model and irrigation scheme

This study is based on the system developed by Modanesi et al. (2022) in which the Noah-MP LSM version 3.6 (Niu et al., 2011), equipped with a sprinkler irrigation module (Ozdogan et al., 2010), is run within the NASA Land Information System (LIS) version 7.4 (Kumar et al., 2006, 2008). The LSM has four soil layers corresponding to the following depths: 0-10 cm (surface soil moisture; SSM), 10-40 cm (SM1), 40-100 cm (SM2), and 100-200 cm (SM3).

The irrigation scheme, coupled to the Noah-MP LSM, was initially developed by Ozdogan et al. (2010) and based on a soil moisture deficit approach. In the case of a fully irrigated pixel, the irrigation scheme depends on two conditions for irrigation to be triggered: (1) the day must fall within the growing season, and (2) the rootzone soil moisture must reach a certain depletion. First, the growing season is defined by a greenness vegetation fraction (GVF [-]) threshold,  $GVF_{irr}$ , as suggested by Ozdogan et al. (2010):

$$GVF_{irr} = GVF_{min} + 0.4 * (GVF_{max} - GVF_{min}) \quad (1)$$

In this study, GVF is based on a monthly climatology, and  $GVF_{min}$  and  $GVF_{max}$  are respectively the minimum and maximum monthly GVF. Second, the soil must be dry enough, meaning that the rootzone soil moisture has to reach a certain depletion. In the irrigation scheme, the depletion is defined by the moisture availability ( $MA$  [-]) as follows:

$$MA = \frac{\sum_{l=1}^{l_{root}} \theta_l * RD_l - \sum_{l=1}^{l_{root}} \theta_{PWP} * RD_l}{\sum_{l=1}^{l_{root}} \theta_{FC} * RD_l - \sum_{l=1}^{l_{root}} \theta_{PWP} * RD_l} \quad (2)$$

where  $\theta_l$  [-] and  $RD_l$  [m] are the soil moisture content and rooting depth of the  $l^{th}$  soil layer, and  $\theta_{PWP}$  [-] and  $\theta_{FC}$  [-] are the water contents at permanent wilting point and field capacity of the corresponding soil texture. The considered soil layers in the computation of  $MA$  vary over the growing season given that  $RD$  directly depends on the GVF, i.e.

$$RD = GVF * RD_{max} \quad (3)$$

in which  $RD_{max}$  [m] is the maximum rooting depth (a vegetation parameter), and GVF is based on a monthly climatology (as in Equation 1). When both conditions (growing season and dry soil) are fulfilled, irrigation is triggered and the amount of water required brings the rootzone soil moisture back to field capacity. The irrigation rate ( $Irr_{rate}$  [mm s<sup>-1</sup>]) is then defined as follows:

$$Irr_{rate} = \frac{\sum_{l=1}^{l_{root}} (\theta_{FC} - \theta_l) * RD_l * 1000}{Irr_{time}} \quad (4)$$

where the  $Irr_{time}$  (in seconds) corresponds to the period when irrigation is allowed. This time frame is set to 06:00 to 10:00 LT following Ozdogan et al. (2010). The  $Irr_{rate}$  is then added to the precipitation at each model time step. In our study, we report the total irrigation amount per day, which is effectively applied at each model time step within the 4-hour irrigation period.

### 2.2 Nature run and synthetic observations

The Noah-MP with irrigation module was used to create a nature run (also called the ‘truth’) that provides reference data of soil moisture, LAI, and irrigation, along with all other variables. This output was also used to generate synthetic  $\gamma_{VV}^0$  observations (via a calibrated WCM) that were assimilated in the different synthetic DA experiments.

206 The model was run at a temporal resolution of 15 min and at a  $0.01^\circ \times 0.01^\circ$  lat-lon  
 207 spatial resolution, and the results are only shown for a single sandy loam pixel that is fully  
 208 irrigated in Italy ( $44.565^\circ\text{N}$ ,  $11.525^\circ\text{E}$ ). The scientific findings are the same for any pixel  
 209 in this synthetic study, and our setup can be readily expanded to a large domain. Mete-  
 210 orological data to force the nature run were extracted from the Modern-Era Retrospective  
 211 analysis for Research and Applications version 2 (MERRA2; Gelaro et al., 2017), which were  
 212 remapped from a spatial resolution of  $0.5^\circ \times 0.625^\circ$  to the resolution of this study by bilinear  
 213 interpolation. Soil texture parameters were taken from the 1 km Harmonized Soil World  
 214 Database (HWSD v1.21). Irrigation was triggered when the  $MA$  reached 0.45. This nature  
 215 simulation ran over the period from 2010 through end 2019 after a model spin-up starting  
 216 on 1 January 2000. Based on the GVF climatology ( $0.144^\circ$  spatial resolution; Gutman &  
 217 Ignatov, 1998) at this location, the growing season was defined as the months covering April  
 218 through September.

219 Synthetic  $\gamma_{VV}^0$  observations were generated daily (at 06:00 LT) from the nature run by  
 220 propagating the SSM and LAI estimates through a calibrated WCM, which is considered  
 221 to be perfect ('*true*'), just like the LSM, in this synthetic study. The WCM describes the  
 222 soil and vegetation scattering processes through semi-empirical formulas (Attema & Ulaby,  
 223 1978) and therefore uses SSM and LAI from the LSM to simulate backscatter. The WCM  
 224 calibration was based on input from a model simulation with irrigation simulation activated  
 225 and real S1 backscatter observations, following Modanesi et al. (2021, 2022). The synthetic  
 226 observations are assimilated after perturbing them with different levels of Gaussian white  
 227 noise, with standard deviations ranging from 0 to 0.7 dB (see Section 2.3).

## 228 **2.3 Experiments**

### 229 **2.3.1 Model-only run**

230 An overview of all experiments is given in Figure 1. Model-only runs, also called  
 231 open-loop (OL), were performed with the same settings and inputs as the nature run, but  
 232 with an introduction of forcing error. Specifically, the meteorological forcings were altered  
 233 in two different ways: (1) all forcings were kept identical to the nature run (MERRA2)  
 234 except for precipitation which was shifted in time (using 2000-2009, instead of 2010-2019),  
 235 referred to as  $OL_H$  (high forcing error); and (2) all MERRA2 forcings were replaced with  
 236 the European Center for Medium-Range Weather Forecasts (ECMWF) Reanalysis version 5  
 237 (ERA5; Hersbach et al., 2020), referred to as  $OL_M$  (mild forcing error). For the first case,  
 238 shifting the MERRA2 precipitation (also performed by Giroto et al., 2021) introduces long-  
 239 term errors since the interannual variability of the precipitation deviates from the truth. By  
 240 contrast, the experiments with mild forcing errors will use monthly and annual precipitation  
 241 patterns that are closer to the truth and the errors mostly represent short-term deviations.  
 242 The OL experiments served as a reference to assess the skill gain of the DA experiments.

### 243 **2.3.2 Default DA experiments**

244 In the default DA experiments ( $DA_1$ ), daily synthetic  $\gamma_{VV}^0$ , without any addition of  
 245 noise, are assimilated to update the SSM at all update time steps. The irrigation scheme is  
 246 primarily triggered by the (updated) soil moisture deficit, similar to the OL. In line with the  
 247 OL simulations, the  $DA_1$  experiments were also run for a high ( $DA_{1,H}$ ) and mild ( $DA_{1,M}$ )  
 248 forcing error. The aim of  $DA_1$  is to identify the strengths and weaknesses of the approach  
 249 by Modanesi et al. (2022).

### 250 **2.3.3 Buddy check DA experiments**

251 The last series of experiments aim at testing the newly proposed buddy check approach  
 252 ( $DA_2$ ) described in Section 2.4.2. Similar to above, the DA was tested for setups of forcing  
 253 error, i.e.  $DA_{2,H}$  and  $DA_{2,M}$ . The method was tested for daily perfect (no white noise)

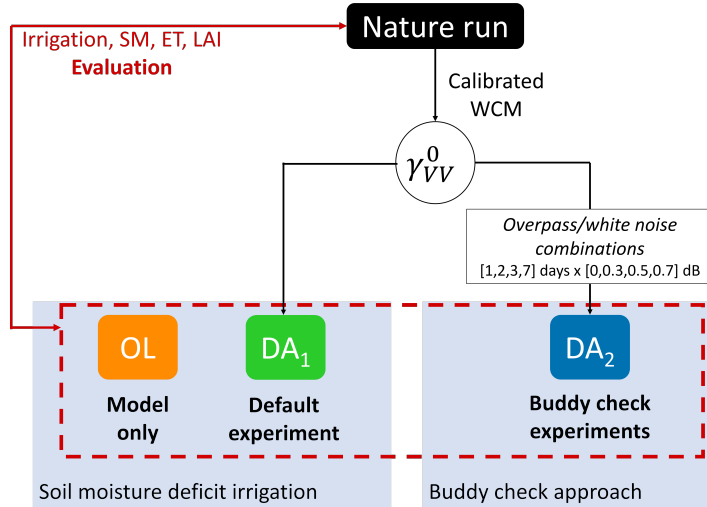


**Figure 1.** Overview of the experiments. Note that all experiments are repeated for high forcing error ( $OL_H$ ,  $DA_{1,H}$ ,  $DA_{2,H}$ ) and mild forcing error ( $OL_M$ ,  $DA_{1,M}$ ,  $DA_{2,M}$ ).

254 observations, as well as for different overpass intervals (one observation every 1, 2, 3, and 7  
 255 days), and different white noise levels in the assimilated observations. White noise is added  
 256 to the observations in time through a Gaussian distribution of mean zero and different  
 257 standard deviations ( $\sigma$ ): 0, 0.3, 0.5, and 0.7 dB. This range in total observation error  
 258 (measurement+representativeness error) was chosen considering the fact that the S1 CSAR  
 259 instruments on board of S1-A and S1-B have respective radiometric accuracies ( $1\sigma$ ) of  
 260 0.25 dB and 0.32 dB (varying with the acquisition mode and polarization; Miranda et al.,  
 261 2017) and that the observation operator is assumed to be perfectly calibrated (i.e. the  
 262 calibrated WCM is the truth), which limits the representativeness error (van Leeuwen,  
 263 2015). Note that when white noise was added to the signal, experiments were run for three  
 264 different seeds of random noise.

### 265 2.3.4 Ensembles

266 For all experiments (OL,  $DA_1$ , and  $DA_2$ ), a total of 24 ensemble members were used.  
 267 The ensembles were generated by perturbing model forcings (rainfall, incident longwave ra-  
 268 diation, incident shortwave radiation) and the SSM state variable (only, i.e. the uncertainty  
 269 on LAI is assumed to be marginal). For further details on the perturbation parameters,  
 270 the reader can refer to Modanesi et al. (2022). It should be noted that in contrast to the  
 271 setup of Modanesi et al. (2022), a perturbation bias correction method was applied in this  
 272 study. This adjustment was proposed by Ryu et al. (2009) to avoid unintended biases in  
 273 the forecast of soil moisture. To be able to use this option with the soil moisture deficit  
 274 irrigation approach (OL and  $DA_1$ ), the conditions for which irrigation is triggered required  
 275 slight modifications. In the Noah-MP v3.6 LSM, irrigation is triggered by looking at the  $MA$   
 276 of each ensemble member individually. This is not compatible with the perturbation bias  
 277 correction option as the correction can bring the soil moisture of several ensemble members  
 278 sooner to an irrigation state when some other members have not reached the  $MA$  threshold  
 279 yet. Therefore, in this study and for all experiments, irrigation was triggered based on  
 280 the ensemble mean  $MA$  and the same amount of irrigation water (also calculated from the  
 281 ensemble mean) is applied to each ensemble member. This was already corrected in the  
 282 irrigation module of the latest Noah-MP version (4.0.1).

## 2.4 Data assimilation

### 2.4.1 State updating

Synthetic observations of co-polarized backscatter ( $\gamma_{VV}^0$ ) were assimilated to update the SSM, and all other variables via model propagation. An ensemble Kalman filter (EnKF) was employed to ingest  $\gamma^0$  observations into an erroneous version of the Noah-MP LSM (i.e. different from that of the nature run, see Section 2.3). The 24 ensemble members were used to derive the forecast error. The ‘true’ calibrated WCM was used as observation operator to produce observation predictions based on the erroneous LSM simulations of SSM and LAI. The update equation of the EnKF can be written as follows:

$$\widehat{x}_i^{\dagger} = \widehat{x}_i^{-} + K_i[y_{obs,i} - h_i(\widehat{x}_i^{-})] \quad (5)$$

for which  $\widehat{x}_i^{\dagger}$  is an ensemble of the updated model states at time step  $i$ ,  $\widehat{x}_i^{-}$  is the ensemble forecast state,  $y_{obs,i}$  is the assimilated observation ( $\gamma_{VV}^0$ ),  $K_i$  is the Kalman gain, and  $h_i(\cdot)$  is the WCM observation operator. The innovation at time  $i$  ( $innov_i$ ) is defined as the residual between the observed and the forecast  $\gamma_{VV}^0$  and is expressed in decibels (dB):

$$innov_i = y_{obs,i} - h_i(\widehat{x}_i^{-}) \quad (6)$$

Even though the observation predictions use both SSM and LAI as input, the update is limited to SSM here for simplicity (unlike Modanesi et al., 2022).

### 2.4.2 Buddy check approach

Because Modanesi et al. (2022) reported that DA updates to a wetter soil moisture could possibly lead to missed simulated irrigation events, we tested a novel approach in this study, illustrated in Figure 2 for a case with daily observations. We still update SSM as proposed above. However, the triggering of irrigation is now not merely based on a modeled soil moisture deficit, but instead always requires a high positive difference between the observed and forecast  $\gamma_{VV}^0$  (innovation; Equation 6). In other words, the timing of the irrigation is now primarily observation-based. The new method builds on a simple buddy check approach, commonly used in atmospheric DA (e.g., Dee et al., 2001), avoiding the assimilation of outlier observations. In this case, outliers are detected when the innovation is suddenly large and positive, corresponding to a significantly higher observed than forecasted  $\gamma_{VV}^0$  (highlighted blue dots in Figure 2a). This ‘jump’ in the innovations can be detected by looking at the difference between two successive innovations. This will be referred to as  $\Delta innov_i$ , defined as:

$$\Delta innov_i = innov_i - innov_{i-T} \quad (7)$$

where  $T$  is the overpass time interval [days]. For an observation to be detected as an outlier,  $\Delta innov_i$  should be larger than a certain threshold, expressed in dB. The latter is chosen to be adaptive, i.e. a multiple of the standard deviation of the innovations ( $SD_{innov,n}$ ) computed on the antecedent  $n$  days. The choice was made to dynamically compute  $SD_{innov,n}$  with a moving window to account for the natural variability of the model and observation errors, and thus the innovations. In this study, the buddy check approach was tested for two different window sizes, i.e. windows of 20 ( $SD_{innov,20}$ ) and 60 days ( $SD_{innov,60}$ ) were considered. The outlier detection is illustrated in Figure 2b.

A strong positive innovation (outlier) hints towards an unmodeled process, i.e. irrigation. Therefore, when an outlier is detected at day  $i$ , irrigation can be triggered but only when the conditions required for irrigation are met: (1) the day  $i$  has to fall in the growing season, and (2) the  $MA$  should be lower than a certain threshold to avoid unrealistic irrigation events (when the soil is too wet). The latter threshold is set to 0.50 and is slightly

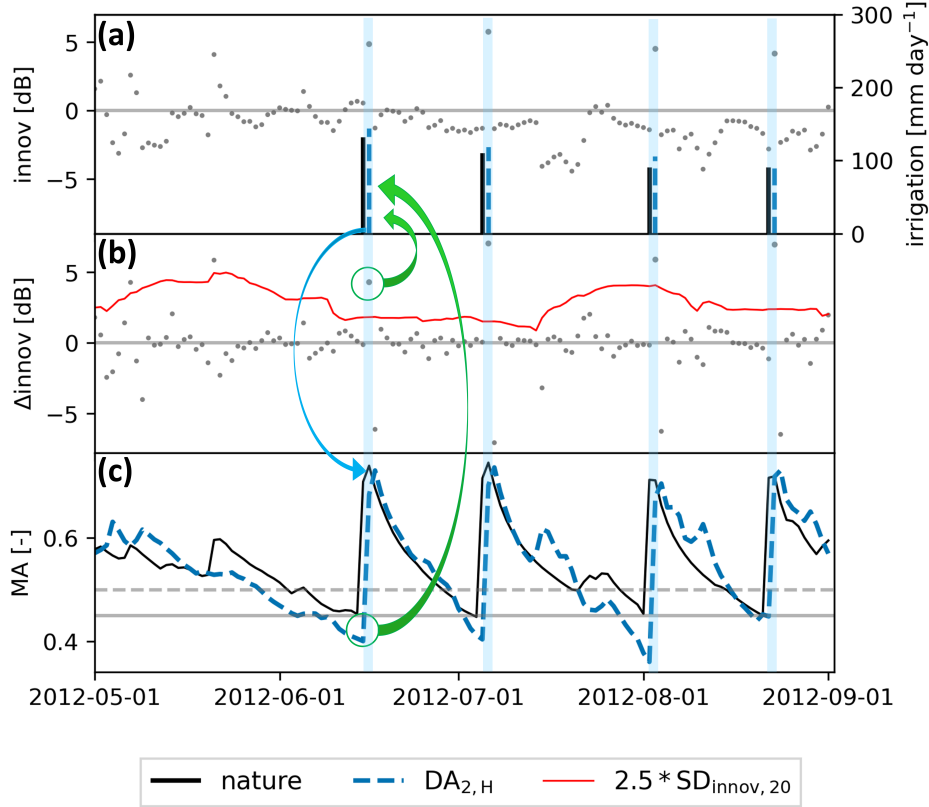


**Figure 2.** Illustration of the buddy check approach. (a) Irrigation time series [ $\text{mm day}^{-1}$ ] of the nature run and the DA run with buddy check approach with the innovations [dB] in grey. (b)  $\Delta_{\text{innov}}$  [dB] time series with the dynamic threshold (based on a 20-day window,  $2.5 * SD_{\text{innov},20}$ ). (c) Moisture availability ( $MA$  [-]) of the nature run and the DA buddy check run and the corresponding thresholds: 0.45 fixed threshold for irrigation for the nature run, 0.50 upper threshold to allow irrigation for the buddy check approach. The shaded blue stripes highlight the irrigation events. The green arrows illustrate the two conditions required to simulate irrigation. The blue arrow links the irrigation event to the increase in  $MA$ .

321 relaxed compared to the truth's 0.45 value to give way to an observation-based trigger, e.g.  
 322 when a farmer would irrigate before the uncertain model reaches a critical  $MA$ . Further-  
 323 more, unlike the nature (or OL or DA<sub>1</sub> case), the DA<sub>2</sub> approach allows the  $MA$  to decrease  
 324 freely, mimicking the reality that farmers might sometimes irrigate later than expected. The  
 325 condition on the  $MA$  is illustrated by Figure 2c. For each irrigation event, the rootzone soil  
 326 moisture is increased to field capacity, corresponding to  $MA=1$ . However, this is not visible  
 327 in  $MA$  time series (Figure 2c) as the plotted  $MA$  is computed based on the daily averaged  
 328 soil moisture contents. For days in the growing season (from April through September for  
 329 the climatological GVF), the conditions to trigger irrigation can thus be summarized as  
 330 follows:

$$\begin{cases} \Delta_{\text{innov}_i} \geq 2.5 * SD_{\text{innov},n} \\ MA_i \leq 0.50 \end{cases} \quad (8)$$

331 In short, an outlier innovation is not used to update the soil moisture state, but to correct  
 332 the model input by adding water as irrigation. The amount of irrigation water is computed

333 by the irrigation scheme coupled to the Noah-MP LSM described in Section 2.1, and it  
 334 benefits from the updated soil moisture prior to the irrigation trigger. It is important to  
 335 note that this method was implemented in the LIS framework itself, allowing an online  
 336 modeling of irrigation with this approach. However, since irrigation starts at 6:00 LT in the  
 337 irrigation scheme, and the synthetic  $\gamma_{VV}^0$  observations were produced at the same time of  
 338 the day, irrigation is not yet part of the observations when they are checked for assimilation  
 339 (and either assimilated or flagged as outlier): the irrigation of day  $i$  is only visible in the  
 340 observation of day  $i + 1$  (see Figure 2). Hence, with this buddy check approach, irrigation  
 341 events are always delayed compared the truth. This technical detail is tied to observation  
 342 and irrigation times, and could be overcome via postprocessing or model rewinding in the  
 343 future.

## 344 2.5 Evaluation metrics

345 The experiments were evaluated in terms of irrigation, soil moisture, ET, and LAI.  
 346 Soil moisture was assessed for the different layers (SSM, SM1, SM2, SM3) as defined in  
 347 Section 2.1. The metrics used in this study to evaluate these variables are the Pearson  
 348 correlation (R), the bias, and the root-mean-square difference (RMSD), and are defined as  
 349 follows:

$$R = \frac{\sum_{n=1}^N (x_n - \bar{x})(y_n - \bar{y})}{\sqrt{\sum_{n=1}^N (x_n - \bar{x})^2 \sum_{n=1}^N (y_n - \bar{y})^2}} \quad (9)$$

$$bias = \frac{1}{N} \sum_{n=1}^N (x_n - y_n) \quad (10)$$

$$RMSD = \sqrt{\frac{1}{N} \sum_{n=1}^N (x_n - y_n)^2} \quad (11)$$

350 where  $x$  is the value of the simulated land surface variable from the OL or DA experiment,  $y$   
 351 is the reference value (from the nature run), and  $N$  are the number of reference data in time  
 352 ( $n = 1, \dots, N$ ).  $\bar{x}$  and  $\bar{y}$  represent the temporal mean values. For LAI, the R is computed  
 353 on the anomalies ( $anomR$ ), because this land surface variable has a clear climatological  
 354 pattern and naturally results in high R values.

355 The normalized information contribution in R ( $NIC_R$ ) and RMSD ( $NIC_{RMSD}$ ) is com-  
 356 monly used to describe the improvement or degradation of the estimates compared to a  
 357 model only (OL) run:

$$NIC_R = \frac{R_{DA} - R_{OL}}{1 - R_{OL}} \quad (12)$$

$$NIC_{RMSD} = \frac{RMSD_{OL} - RMSD_{DA}}{RMSD_{OL}} \quad (13)$$

358 Positive NIC values correspond to an improvement while a negative NIC indicates poorer  
 359 estimations than those of the OL.

360 Irrigation is evaluated with the same metrics on a daily basis, but also considering  
 361 different levels of smoothing where the antecedent  $n$  daily irrigation amounts are averaged.  
 362 Smoothing windows of different lengths ( $n$  days) are considered to better grasp for which  
 363 time intervals (e.g., daily, weekly, monthly) the irrigation events can be accurately simulated.  
 364 Additionally, binary metrics are considered to assess the performance to detect (in terms of

365 timing) the irrigation events. The probability of detection (POD) and the false alarm ratio  
 366 (FAR) are computed on a daily basis and were defined by Roebber (2009) as follows:

$$POD = \frac{TP}{TP + FN} \quad (14)$$

$$FAR = \frac{FP}{TP + FP} \quad (15)$$

367 where TP, FN, and FP are the true positive (detected), false negative (missed), and false  
 368 positive (false) irrigation events. Both metrics range from 0 to 1 and should be equal to 1  
 369 and 0 for the POD and FAR, respectively, in an ideal case. Note that POD and FAR were  
 370 computed on the daily irrigation estimates  $\pm 1$  day, therefore accounting for the technical  
 371 delay of irrigation with the buddy check approach (see Section 2.4.2).

### 372 3 Results

#### 373 3.1 DA<sub>1</sub>: soil moisture updating can limit irrigation estimation

374 In the default DA experiments (DA<sub>1</sub>), irrigation is primarily triggered when the modeled  
 375 (or analysis) soil moisture deficit exceeds a threshold. The results are first presented for  
 376 the DA<sub>1,H</sub>, for which daily  $\gamma_{VV}^0$  observations without noise were assimilated into a model  
 377 forced by precipitation taken from another time period than the truth. Figure 3a illustrates  
 378 some irrigation events of the nature run ('truth'), OL<sub>H</sub>, and DA<sub>1,H</sub> along with the  $\gamma_{VV}^0$   
 379 innovations. The corresponding MA time series are shown in Figure 3b with the threshold  
 380 that needs to be reached to trigger irrigation (0.45). First, it can be seen that the assimilation  
 381 of  $\gamma_{VV}^0$  observations brings the soil moisture, and consequently the MA, to a state that is  
 382 closer to the nature run, moving the first irrigation event (in June) closer to the nature  
 383 run compared to the OL. In contrast, the last irrigation event (in August) does not occur  
 384 in the DA<sub>1,H</sub>. The MA of DA<sub>1,H</sub> does not reach the 0.45 threshold before the true event  
 385 and the irrigation simulation is consequently prevented by updates to wetter soil moisture  
 386 conditions as a result of large positive innovations (Figure 3).

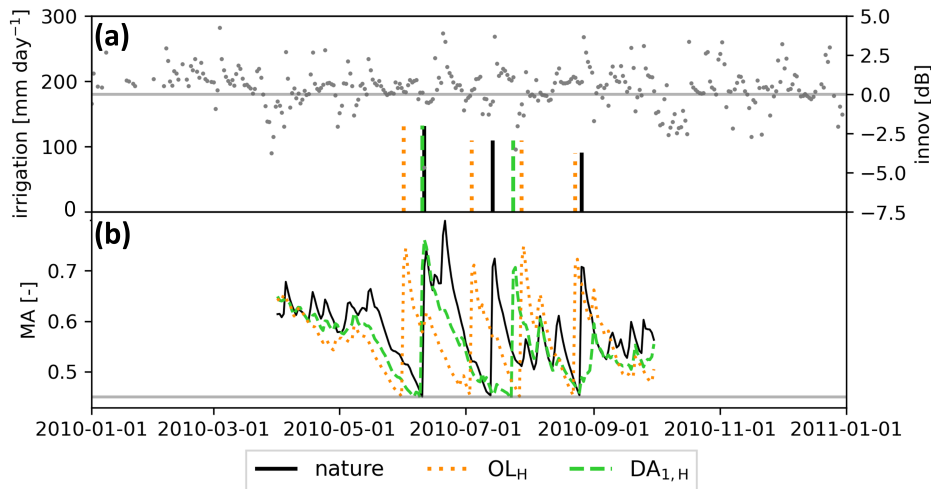


**Figure 3.** (a) Time series of the irrigation [ $\text{mm day}^{-1}$ ] of the nature run, OL<sub>H</sub>, and DA<sub>1,H</sub>. The grey dots correspond to the  $\gamma_{VV}^0$  innovations. (b) Time series of the corresponding moisture availability (MA [-]) for the irrigation months (April through September) along with the corresponding threshold to trigger irrigation (grey line).

387 More generally, over the 10-year experiment, the DA irrigation events that are not es-  
 388 timated before the true irrigation are typically delayed or skipped, similar to what can be  
 389 observed for July and August in Figure 3. For the 10-year period, the daily irrigation esti-  
 390 mates  $\pm 1$  day have low POD values of 0.40 and 0.43 for  $DA_{1,H}$  and  $DA_{1,M}$ , respectively.  
 391 The system compensates for the lack of water in the soil through positive soil moisture  
 392 increments instead of an irrigation application based on an improved initial condition. Fig-  
 393 ure 4 presents the effect of the assimilation on irrigation estimates in terms of NIC values  
 394 for both forcing error ( $DA_{1,H}$  and  $DA_{1,M}$ ), along with the absolute metrics for the OL.  
 395 Daily irrigation was smoothed for different window sizes before computing the  $NIC_R$  and  
 396  $NIC_{RMSD}$ . For the  $DA_1$  experiments (green), NIC values are positive for most smoothing  
 397 intervals and peak when irrigation is smoothed over a 14-day window. However, the NIC  
 398 metrics drop to negative values for  $DA_{1,M}$  starting from a bimonthly smoothing. This can  
 399 be explained by the difference in forcings. The ERA5 meteorology follows the seasonal  
 400 patterns of the MERRA2 meteorology used for the truth, therefore the seasonal amount of  
 401 irrigation from a model-only  $OL_M$  run is close to the nature, as indicated by the high R and  
 402 low RMSD values, especially for the longer aggregation windows in Figure 4c and d. The  
 403 effect of (sometimes erroneous) irrigation estimation on other land surface variables is later  
 404 discussed in Section 3.2.3.

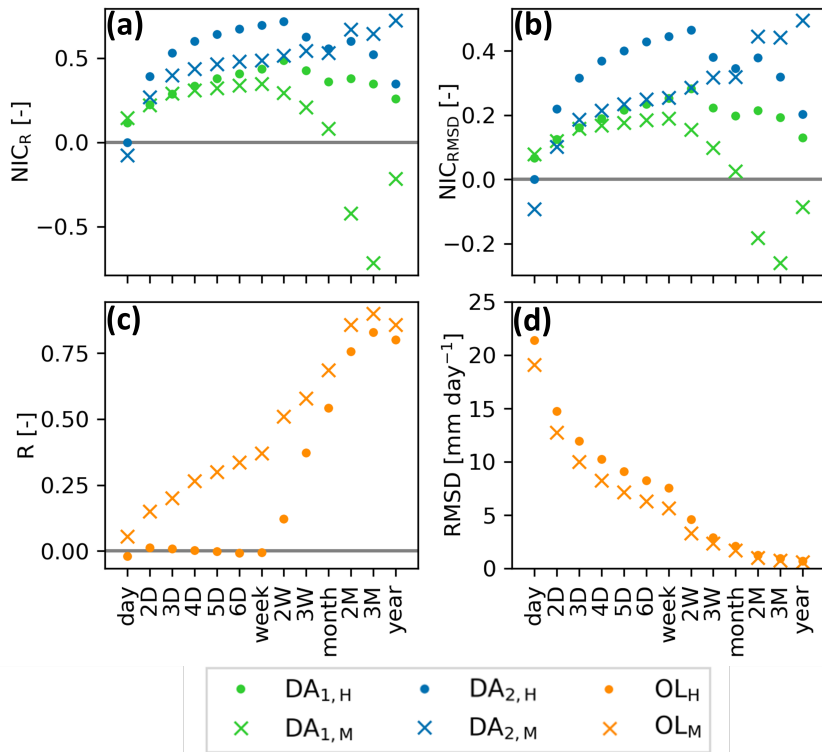


**Figure 4.** (a)  $NIC_R$  [-] and (b)  $NIC_{RMSD}$  [-] for irrigation smoothed with different window sizes. (c) Pearson  $R$  [-] and (d)  $RMSD$  [ $mm\ day^{-1}$ ] of the OL. The dots and the crosses correspond to the high and mild forcing error experiments, respectively.  $DA_2$  were performed by assimilating daily perfect observations. All metrics were computed on the irrigation months only (April through September) over the 10-year experiment.

405 The missed or delayed irrigation events can be identified in the innovation time series.  
 406 Large innovations occur on true irrigation days (Figure 3a), highlighting that a process is  
 407 missed by the model. Instead of avoiding or delaying the event in a DA run, the newly

408 proposed buddy check approach, for which the results are described in the next section, can  
 409 identify and trigger such irrigation events.

### 410 3.2 DA<sub>2</sub>: new buddy check approach

#### 411 3.2.1 Assimilation of daily perfect backscatter observations

412 The results of the new buddy check approach are first presented for daily assimilation  
 413 of observations without white noise and using a 20-day window to compute the outlier  
 414 threshold ( $SD_{innov,20}$ ). Figure 5 shows the innovations and irrigation results of DA<sub>2,H</sub>  
 415 for the period 2010-2015 (panel a), with the associated MA time series for 2010 in panel b. The  
 416 DA<sub>2,H</sub> irrigation estimates (dashed blue bars) capture most of the true irrigation events (full  
 417 black lines). During these five years, one event is missed at the end of the irrigation season  
 418 in 2013. This can be explained by (intentionally) erroneous rainfall events in the DA run,  
 419 causing soil moisture that is higher than the irrigation threshold ( $MA > 0.5$ ). On the other  
 420 hand, two false irrigation events are simulated. Both can be attributed to rainfall events in  
 421 the nature run, leading to an occasional large positive innovation, and since the moisture  
 422 conditions are dry enough, irrigation is consequently triggered. This proves that when the  
 423 forcings are erroneous (i.e. rainfall is missed in the DA run), irrigation cannot be dissociated  
 424 from rainfall in the  $\gamma_{VV}^0$  signal.

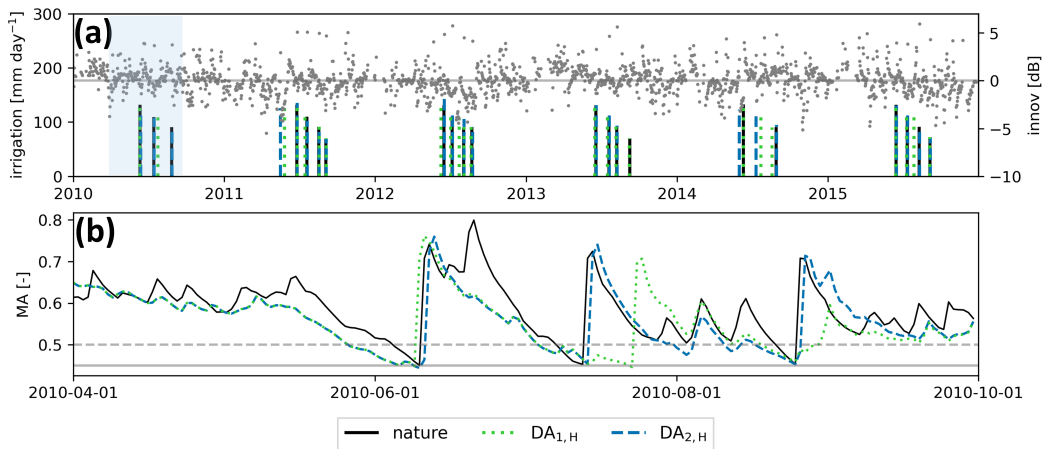


**Figure 5.** (a) Time series of the irrigation [mm day<sup>-1</sup>] of the nature run, DA<sub>1,H</sub>, and DA<sub>2,H</sub> for daily observations without noise and an outlier threshold based on  $SD_{innov,20}$ . Innovations of DA<sub>2,H</sub> are shown in the background in grey. (b) Time series for the growing season of 2010 (shaded in blue in a) of the moisture availability ( $MA$  [-]) of the nature run, DA<sub>1,H</sub>, and DA<sub>2,H</sub> for the irrigation months (April through September). In (b), the dashed grey line corresponds to the maximum allowable  $MA$  for irrigation for DA<sub>2,H</sub> (0.50) and the full line is the threshold for the nature run and DA<sub>1,H</sub> (0.45).

425 Over the whole 10-year experiment, irrigation estimates are strongly improved by the  
 426 implementation of the buddy check approach, raising the POD of the daily irrigation esti-  
 427 mates  $\pm 1$  day from 0.40 for DA<sub>1,H</sub> to 0.86 for DA<sub>2,H</sub>, and from 0.43 for DA<sub>1,M</sub> to 0.80  
 428 for DA<sub>2,M</sub>. For both forcing errors, the FAR is about 0.17, which is also an improvement  
 429 compared to the values for DA<sub>1,H</sub> (0.60) and DA<sub>1,M</sub> (0.42). Figure 4 shows the  $NIC_R$   
 430 and  $NIC_{RMSD}$  for the different irrigation smoothing windows for DA<sub>2,H</sub> and DA<sub>2,M</sub> (daily  
 431 assimilation without noise). Unlike DA<sub>1</sub>, the  $NIC$  values for all DA<sub>2</sub> experiments remain  
 432 above the zero-line, meaning that irrigation estimates are improved for all smoothing inter-  
 433 vals, relative to the OL. Starting from a 3-day smoothing interval, R and RMSD values are

434 improved by more than 30% and 10%, respectively, for all forcing errors and smoothing inter-  
 435 vals. NIC values tend to drop for  $DA_{2,H}$  for longer aggregation levels as a consequence of  
 436 the occasional false or missed irrigation events. The poor effect on irrigation quantification  
 437 at a daily scale can be attributed to the timing of the observation and irrigation application  
 438 (see Section 2.4.2).

### 439 **3.2.2 Effect of observation interval and white noise**

440 The buddy check implementation was tested for different observation intervals (1, 2, 3,  
 441 and 7 days) and observation noise levels (0, 0.3, 0.5, and 0.7 dB), to assess which observation  
 442 configuration would be ideally suited for irrigation estimation. The 14-day smoothed daily  
 443  $DA_2$  irrigation estimates are evaluated relative to the OL through the  $NIC_R$  and  $NIC_{RMSD}$ .  
 444 The bias (difference between the daily simulated and nature irrigation) is also assessed to  
 445 indicate if there is a general over- or underestimation of the irrigation amounts. The results  
 446 for the  $DA_{2,H}$  and  $DA_{2,M}$  experiments are shown in Figure 6. Two thresholds were tested  
 447 to trigger irrigation, using two different window sizes for the calculation of  $SD_{innov}$ : 20 days  
 448 ( $SD_{innov,20}$ ), and 60 days ( $SD_{innov,60}$ ). Note that the experiments assimilating observations  
 449 with a 7-day interval could only be performed with a 60-day window in order to compute  
 450 a standard deviation with enough data points. All experiments with white noise in the  
 451 observation signal were performed for three random seeds of added noise and the average  
 452 metric is presented.

453 The performance of the buddy check approach degrades with longer observation inter-  
 454 vals, to reach marginal improvements for the  $DA_{2,H}$ , and even poorer irrigation estimations  
 455 for the  $DA_{2,M}$  than for  $OL_M$  (Figure 6a,b,d,e). Less frequent observations lead to stronger  
 456 underestimations of the irrigation amounts, as shown by the negative biases (Figure 6f).  
 457 In the worst scenario for  $DA_{2,H}$  (7-day observation interval with noise), about half of the  
 458 true irrigation water is missing over the 10 years. Even though  $DA_2$  misses more irrigation  
 459 for larger observation intervals compared to the OL, the timing of the remaining detected  
 460 irrigation events is closer to the truth.

461 The white noise in the signal mainly affects the performance when observations are  
 462 frequently available (daily or once every 2 days) for  $DA_{2,H}$  (Figure 6). Similar to the  
 463 effect of a longer observation interval, noise in the signal tends to cause underestimations  
 464 of irrigation amounts. White noise sometimes amplifies the increase in  $\Delta_{innov}$ , making an  
 465 outlier easier to detect, and at other times, the noise reduces the ‘jump’ effect, making the  
 466 event undetectable. Observation noise also increases the risk of detecting a false irrigation  
 467 event. The combination of these three effects reduces the skill of the buddy check approach.  
 468 For reasonable levels of noise ( $\leq 0.5$  dB; Figure 6e), the RMSD is reduced by at least 30%  
 469 when assimilating frequent observations, for both forcing errors.

470 Increasing the window size for the computation of the  $SD_{innov}$  improves the R and  
 471 RMSD for  $DA_{2,M}$ . However, it leads to irrigation underestimation (negative bias) for non-  
 472 daily observations, especially in the case of the  $DA_{2,H}$  (Figure 6f). More irrigation events  
 473 remain undetected because the  $SD_{innov}$  considers innovations up to 60 days before the  
 474 event. This is problematic, especially at the beginning of the season as the natural varia-  
 475 tion in the innovations is larger in the late winter or spring (wet season), which are then  
 476 considered in the computation of the  $SD_{innov,60}$ . On the other hand, a small window size  
 477 ( $SD_{innov,20}$ ) tends to detect more false irrigation events, keeping the bias closer to zero,  
 478 but not necessarily improving the R and RMSD in terms of irrigation. A window size of  
 479 20 days seems more appropriate, in the sense that this  $SD_{innov}$  should capture the natural  
 480 variation of the innovations which is mainly induced by forcing errors but also vegetation.

481 Overall, NIC values for the  $DA_{2,H}$  are larger than for the  $DA_{2,M}$ , in line with the larger  
 482 forcing errors in  $DA_{2,H}$ . The  $OL_M$  already shows a reasonable performance (Figure 4c,d),  
 483 leaving less space for improvement by the  $DA_{2,M}$ .

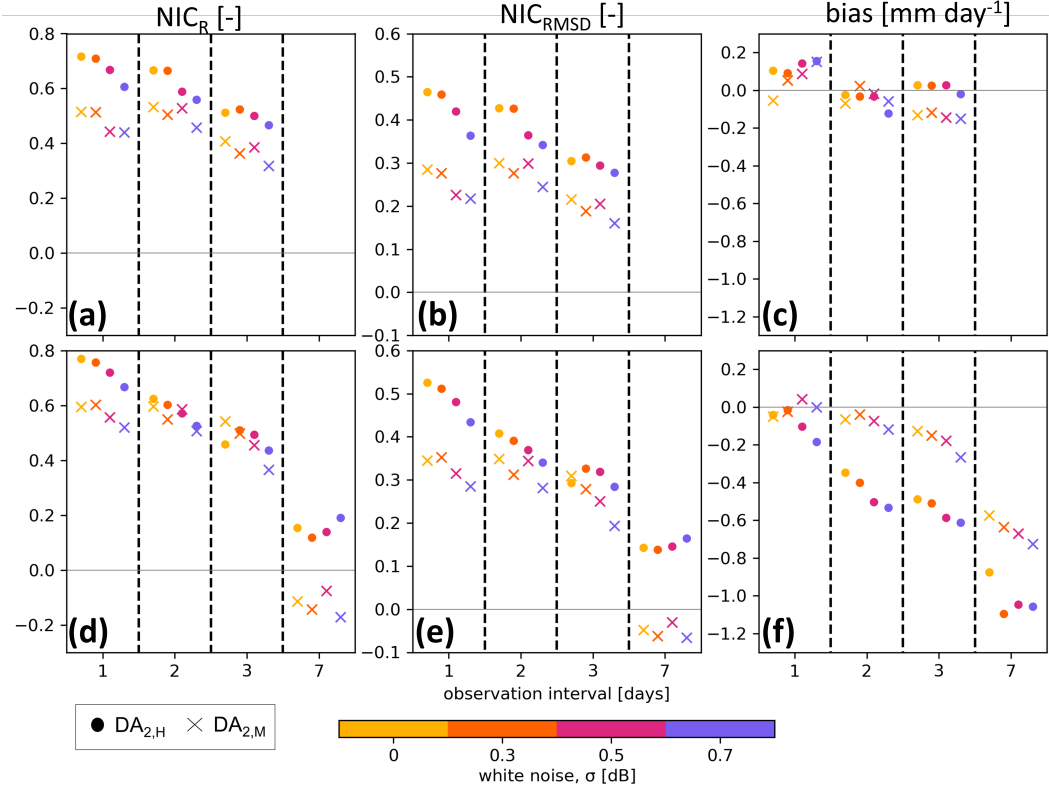


**Figure 6.** (a,d)  $NIC_R$  [-], (b,e)  $NIC_{RMSD}$  [-], and (c,d) bias [ $\text{mm day}^{-1}$ ] of 14-day irrigation amount estimates for the different  $DA_2$ , for 1, 2, 3, and 7-day observation intervals. The colors correspond to the level of Gaussian white noise added to the signal ( $\sigma$ , dB), and for all experiments with noise, the mean metric is taken from the three runs. The rows are associated with the window size taken to compute the standard deviation for the irrigation threshold, where (a,b,c) are based on a 20-day window ( $SD_{innov,20}$ ), and (d,e,f) relate to experiments with a 60-day window ( $SD_{innov,60}$ ). Dots correspond to  $DA_{2,H}$  and crosses to  $DA_{2,M}$ .

### 3.2.3 Impact on other land surface variables

The quality of irrigation estimates has an impact on the other land surface variables. Table 1 shows the R values between daily results for selected OL and DA experiments, relative to the truth. The  $DA_2$  results are shown for an outlier threshold based on  $SD_{innov,60}$  (with irrigation underestimation, Figure 6f) to include the experiments for which weekly observations are assimilated. First, the difference between the two forcing errors is reflected in the significantly lower R values for  $OL_H$  than for  $OL_M$ . For  $DA_2$ , it can be noticed that the novel buddy check approach using daily observations without noise ( $DA_2$  1 day, 0 dB) performs best and is clearly superior to the  $DA_1$  (with daily, perfect observations). The R values of the  $DA_2$  with a 3-day interval and 0.5 dB observation noise are close to those of the  $DA_1$  for both the high and mild forcing error experiments. In the worst case evaluated in this study (7-day interval and 0.7 dB of noise), the performance remains better than the OL when forcings are strongly altered ( $DA_{2,H}$ ), but under the same circumstances, the new method degrades the land surface estimates when forcings are only slightly changed ( $DA_{2,M}$ ).

**Table 1.** R for the SSM, SM1, SM2, SM3, ET, and anomR for LAI, for selected experiments calculated on the entire 10-year experiment. All DA<sub>2</sub> were performed with the  $SD_{innov,60}$  threshold.

	SSM	SM1	SM2	SM3	ET	LAI anomR [-]
	R [-]					
<b>High forcing error</b>						
OL	0.32	0.26	0.34	0.49	0.80	-0.12
DA <sub>1</sub>	0.60	0.60	0.68	0.76	0.86	0.21
DA <sub>2</sub> 1 day, 0 dB	0.70	0.73	0.79	0.79	0.89	0.31
DA <sub>2</sub> 3 day, 0.5 dB	0.56	0.53	0.57	0.65	0.83	0.17
DA <sub>2</sub> 7 day, 0.7 dB	0.49	0.45	0.52	0.60	0.78	-0.01
<b>Mild forcing error</b>						
OL	0.73	0.69	0.71	0.82	0.88	0.71
DA <sub>1</sub>	0.82	0.81	0.81	0.89	0.91	0.78
DA <sub>2</sub> 1 day, 0 dB	0.86	0.84	0.88	0.93	0.92	0.88
DA <sub>2</sub> 3 day, 0.5 dB	0.79	0.76	0.79	0.87	0.90	0.84
DA <sub>2</sub> 7 day, 0.7 dB	0.72	0.66	0.66	0.80	0.86	0.60

499 For longer observation intervals, the anomR of LAI reduces significantly in the DA<sub>2</sub>  
500 runs. When irrigation events are missed in the new DA<sub>2</sub> system (e.g. because the next  
501 observation falls too far in time after the irrigation event, making irrigation undetectable  
502 in the signal), there is a risk that LAI starts to drop drastically as a response to a water  
503 shortage in the root zone.

## 504 4 Discussion

### 505 4.1 Novel approach to estimate irrigation in a DA system

506 The synthetic setup in this study helps to optimize the DA design for irrigation quan-  
507 tification. The soil moisture updating via DA can help to improve the initial conditions to  
508 trigger irrigation and to estimate the right amount of irrigation, but a blind ingestion of all  
509 observations can update soil moisture to wetter conditions which already reflect the presence  
510 of irrigation and inhibit irrigation estimation by the model, as in Modanesi et al. (2022).  
511 This phenomenon was illustrated in Figure 3 where irrigation events were delayed or missed  
512 because the required water is compensated by strong positive soil moisture increments. The  
513 idea of the buddy check approach builds on this limitation by preventing these updates to  
514 wetter conditions and forcing irrigation in the model instead. More specifically, the method  
515 relies on the fact that a sudden large difference between the observed and forecasted  $\gamma_{VV}^0$   
516 can only come from an unmodeled process, which corresponds to irrigation in this synthetic  
517 experiment. The primary condition is now the detection of an outlier (observation-based)  
518 and not the soil moisture deficit threshold anymore. This makes the timing of the estimated  
519 irrigation less model-dependent and more in line with actual practices on the field.

520 The new method shows good performances in terms of irrigation estimation when fre-  
521 quent (daily or every other day) observations are available, which corresponds to the initial  
522 revisit interval (2-3 days, location dependent) of the S1 constellation over Europe. Reason-  
523 able performances are still expected for a 3-day observation interval but weekly observations  
524 would not be sufficient to guarantee the irrigation detection skill and lead to severe underes-  
525 timations of irrigation water. The failure of S1-B halved the number of available observations  
526 (one every  $\sim 4$  days in Europe, 12 days elsewhere), making the buddy check approach (used  
527 within a S1 DA system) unsuitable outside of Europe until the launch of the next satellite

(S1-C, expected in the spring of 2023). Other synthetic studies assimilating S1-related SSM products (Abolafia-Rosenzweig et al., 2019; Das et al., in review; Ouadi et al., 2021; Zappa et al., 2022) also highlighted the importance of frequent observations. Zappa et al. (2022) reported large irrigation underestimations when observations are too sparse in time. Similar to our study using  $\Delta_{innov}$  to detect outliers, their approach is based on observed differences in soil moisture ( $\Delta SM$ ). Both methods are observation-based, making them sensitive to observation noise, and to underestimation of the irrigation amounts with less frequent observations, because the irrigation signal fades away in the observations with time. In short, our buddy check approach underestimates irrigation more for infrequent observations or when a large time window is used to compute the  $\Delta_{innov}$  threshold ( $SD_{innov,60}$ ), but the remaining detected irrigation events are identified accurately in time and with the correct amounts of irrigation water.

The main advantages of the new buddy check approach are (1) the flexibility of the outlier detection method to different situations (and different errors), and (2) the relaxation of the model-based soil moisture threshold for irrigation, making the irrigation estimates more in line with what happens in reality (as observed by the satellite). First, the standard deviation of the  $\gamma_{VV}^0$  innovations for the  $DA_H$  and  $DA_M$  experiments reach average values of 1.5 dB and 1 dB, respectively, for the adaptive outlier detection (Equation 8) during the growing season. These values are in line with the magnitude of the expected high and mild forcing errors, with precipitation RMSD values of 5.1 mm day<sup>-1</sup> and 3.6 mm day<sup>-1</sup>, respectively. Consequently, the DA results for both experiments were comparable in terms of NIC. It is expected that the threshold will also adapt to the location (i.e. the soil texture, crop type), which avoids the use of location-dependent thresholds (i.e. a new parameter) for the outlier detection. Second, setting an upper boundary to the  $MA$  to allow irrigation is more realistic than the use of a fixed threshold. For irrigation to be triggered, the threshold can slightly be higher (wetter, up to 0.50 in this case) or much lower (drier). This is more in line with a real world situation where irrigation is not necessarily determined by a fixed soil moisture deficit value, but depends on the agricultural practices and more generally on the water availability.

## 4.2 Limitations and opportunities

The main limitation of the buddy check approach is the missing of irrigation events, esp. for longer observation intervals. To counter this problem, we need frequent satellite data or a hybrid DA system, where the buddy check approach is supplemented with a pure MA-based irrigation model trigger, if the observation interval exceeds the surface soil memory of an irrigation event. The missed irrigation events have the strongest impact on vegetation, with a steep decline in LAI. This issue can be tackled by jointly updating SSM and LAI, as done by Modanesi et al. (2022). Vegetation updating would ask for the assimilation of backscatter in cross-polarization ( $\gamma_{VH}^0$ ) as this signal has shown to be more affected by vegetation (Patel et al., 2006; Vreugdenhil et al., 2018). A joint assimilation of  $\gamma_{VV}^0$  and  $\gamma_{VH}^0$  would require a combination of both innovations in our buddy check method approach.

The newly proposed buddy check approach could also be used to estimate irrigation with other (e.g. particle) filters or other observations than backscatter data. High resolution L-band soil moisture data would be interesting to guide the estimation of irrigation amounts. Such data can be obtained from e.g., downscaled SMOS or AMSR-E with DisPATCh (Malbêteau et al., 2016) or future missions such as the Copernicus ROSE-L (Davidson & Furnell, 2021) and the SMOS-HR (Rodríguez-Fernández et al., 2019). Nevertheless, the outcome would strongly depend on the quality of the retrievals, and an appropriate bias treatment is needed to avoid the attenuation of the irrigation in the signal (Kumar et al., 2015; Kwon et al., 2022). Instead of changing the type of assimilated observations, the buddy check method could also be used in systems with other models, possibly crop models that are originally designed for agriculture, offering new opportunities in such fields of application.

### 4.3 Future real world experiment

The success of a real world DA experiment with the buddy check approach will depend on the observability of irrigation and model-related limitations. First, satellite observations need to be available at high spatial and temporal resolution, and the actual type of irrigation method needs to be detectable. There is a chance that irrigation is applied for consecutive days over different fractions of the observed satellite footprint (one or a few fields receive irrigation per day). In that case, ‘jumps’ in the innovations will not be detected and the backscatter signal is likely to remain high for these consecutive days. Future research is necessary to counter this limitation, or higher resolution input data and observations are needed. Similarly, some types of irrigation will be easy to detect, whereas others not. Punctual large sprinkler events, as simulated in this study, are more easily detectable than e.g., drip irrigation, which is typically applied in smaller amounts and more frequently.

Second, the LSM and WCM are assumed to be perfect in our synthetic study, but the model-related limitations already mentioned in Modanesi et al. (2022) will be important when going to a real world experiment. Concerning the LSM, the quality of the input data is crucial. Erroneous crop rooting depth, soil texture, or irrigation fraction, would automatically lead to a bias in the irrigation amounts since these factors directly influence the volumes of irrigation water (see LSM equations in Section 2.1). Though more flexible than a rigid soil moisture deficit threshold to trigger irrigation, the upper *MA* threshold of the buddy check approach (set to 0.50 in this study) will need some calibration, as this value may vary across regions. Also the reliability of meteorological forcings is essential. As demonstrated by DA<sub>2</sub>, an outlier can occur when there was a true precipitation event that was not included in the forcings of the simulation (Figure 5). When the root zone is dry enough to allow irrigation, these precipitation events (typically larger than 10 mm) cannot be distinguished from an irrigation event in the signal. The observation operator (e.g. WCM) could also pose a limitation, when directly assimilating microwave signals. Rather than calibrating an empirical model, novel machine-learning based observation operators could improve the system (de Roos et al., in review; Rains et al., 2022), but in both cases, the observation operator training might suffer from an inaccurate match between irrigation simulation (and the effect on soil moisture) and irrigation observed in the satellite signals.

## 5 Conclusions

Irrigation detection and quantification are major challenges. New methods based on remote sensing data are now emerging, including the use of microwave observations in combination with models through data assimilation (DA). Modanesi et al. (2022) assimilated Sentinel-1 backscatter observations into the Noah-MP version 3.6, coupled to a sprinkler irrigation scheme. The soil moisture and vegetation state were updated to set better initial conditions to trigger irrigation simulation, but the system also had limitations, esp. when large updates to wetter conditions delayed or completely inhibited the process-based modeling of irrigation events. This hampers the irrigation quantification by the process model.

In this study, we conducted synthetic experiments for the assimilation of backscatter observations ( $\gamma_{VV}^0$ ) to update soil moisture in a system with erroneous meteorological forcings. After illustrating the shortcoming of blindly assimilating all data for state updating, a new method was developed based on a buddy check approach, in which innovation (observation *minus* forecast) outliers are detected and not assimilated. The method still updates the land surface to guarantee the best possible initial conditions to estimate irrigation amounts, but when an outlier in the innovations is detected, an unmodeled process is assumed and the large innovation is not assimilated. Consequently, the ‘missed’ irrigation is triggered, if the rootzone soil moisture is dry and it is a day in the growing season. The new method is now primarily observation-based, and better adapts to the timing of real irrigation events. The threshold value to identify outlier innovations was made dependent on the locally and

631 temporally varying errors in the system. The method was tested for several observation  
 632 intervals (1, 2, 3, and 7 days) and levels of observation noise, added as Gaussian white noise  
 633 of mean zero and variable standard deviations (0, 0.3, 0.5, and 0.7 dB). The main results  
 634 can be summarized as follows:

- 635 1. For biweekly aggregated irrigation estimates, and compared to a model-only run, the  
 636 new DA method reaches 50–80% and 20–50% of improvement in terms of Pearson  
 637 R and RMSD, respectively, when frequent observations (daily or every other day)  
 638 are available. From a 3-day observation interval onward, the performance degrades  
 639 but remains reasonable ( $NIC_R$ : 20–40%,  $NIC_{RMSD}$ : 15–35%), and for weekly obser-  
 640 vations, there is no improvement compared to a model-only run ( $NIC_R$ : -10–10%,  
 641  $NIC_{RMSD}$ : -10–15%).
- 642 2. The largest improvements from the DA can be seen when the forcing error is large  
 643 (strongly altered meteorological forcings) with a maximum performance for a biweekly  
 644 aggregation of irrigation. When forcing errors are mild (meteorological forcings closer  
 645 to the truth), the improvement peaks for the seasonal irrigation estimates.
- 646 3. Observation error has less impact on the irrigation estimations than the observation  
 647 interval. The  $NIC_R$  drops on average by  $\sim 10\%$  when going from perfect observations  
 648 to random noise levels with a standard deviation of 0.7 dB. Noise negatively impacts  
 649 the performance, especially for frequent observations where irrigation events remain  
 650 undetected or false events are encountered.
- 651 4. The DA improves other land surface variables, such as soil moisture, ET, or LAI  
 652 along with the irrigation estimates. However, the DA cannot recover the LAI when  
 653 the assimilated observations are too sparse in time. The LAI drops as a response to  
 654 the dry soil moisture when irrigation events are missed.

655 The adaptive buddy check approach is flexible and offers new opportunities. The  
 656 method was tested for two very different sets of erroneous forcings and the results were  
 657 similar in terms of improvement compared to a model-only run, suggesting that the method  
 658 indeed adapts to different situations. Furthermore, the buddy check approach can easily  
 659 be implemented in other systems: with another assimilated product (high resolution soil  
 660 moisture retrievals) or with another LSM (or a crop model). After this synthetic evaluation  
 661 of the method, the system is ready to be tested in the real world, but future developments  
 662 (e.g. a hybrid observation- and model-based triggering of irrigation, in case of infrequent  
 663 observations) will be required to obtain a mature DA system for irrigation estimation. The  
 664 localized nature of irrigation in space and time asks for high resolution satellite data, ef-  
 665 ficient modeling, and continued DA advances to accurately quantify the most important  
 666 human use of water.

## 667 6 Open Research

668 The new method implemented in the Land Information System version 3.4 will be made  
 669 available on GitHub after acceptance of this paper, along with the output of the synthetic  
 670 experiment runs in the form of netCDF files, that will be published on Zenodo. The code  
 671 and data can be provided during the review process upon request to the author.

672 The LIS parameters and source code are freely available at <https://lis.gsfc.nasa.gov/>  
 673 and <https://github.com/NASA-LIS/LISF>. The MERRA-2 data (Gelaro et al., 2017)  
 674 were obtained from: <https://goldsmr4.gesdisc.eosdis.nasa.gov/data/MERRA2/>. In  
 675 order to access the data, an account at <https://urs.earthdata.nasa.gov/home> is needed.  
 676 The ERA5 data used in this study have been processed and provided by Météo-France.  
 677 Publicly available ERA5 data can be accessed via the Copernicus Climate Data Store at  
 678 <https://cds.climate.copernicus.eu/> (Hersbach et al., 2020).

## Acknowledgments

The research was funded by the Research Foundation – Flanders (FWO; grant no. 1158423N), ESA IRRIGATION+ (contract no. 4000129870/20/I-NB) and internal KU Leuven C1 (C14/21/057). The resources and services used in this work were provided by the VSC (Flemish Supercomputer Center), funded by the FWO and the Flemish government.

## References

- Abolafia-Rosenzweig, R., Livneh, B., Small, E., & Kumar, S. (2019). Soil Moisture Data Assimilation to Estimate Irrigation Water Use. *Journal of Advances in Modeling Earth Systems*, *11*(11), 3670–3690. Retrieved 2022-05-03, from <https://onlinelibrary.wiley.com/doi/abs/10.1029/2019MS001797> (.eprint: <https://onlinelibrary.wiley.com/doi/pdf/10.1029/2019MS001797>) doi: 10.1029/2019MS001797
- Allen, R. G., Pereira, L. S., Raes, D., & Smith, M. (1998). FAO Irrigation and drainage paper No. 56. Rome: *Food and Agriculture Organization of the United Nations*, *56*(97), e156.
- Attema, E. P. W., & Ulaby, F. T. (1978). Vegetation modeled as a water cloud. *Radio Science*, *13*(2), 357–364. Retrieved 2021-02-25, from <https://agupubs.onlinelibrary.wiley.com/doi/abs/10.1029/RS013i002p00357> (.eprint: <https://agupubs.onlinelibrary.wiley.com/doi/pdf/10.1029/RS013i002p00357>) doi: 10.1029/RS013i002p00357
- Bauer-Marschallinger, B., Freeman, V., Cao, S., Paulik, C., Schaufler, S., Stachl, T., ... Wagner, W. (2019, January). Toward Global Soil Moisture Monitoring With Sentinel-1: Harnessing Assets and Overcoming Obstacles. *IEEE Transactions on Geoscience and Remote Sensing*, *57*(1), 520–539. (Conference Name: IEEE Transactions on Geoscience and Remote Sensing) doi: 10.1109/TGRS.2018.2858004
- Bazzi, H., Baghdadi, N., Fayad, I., Charron, F., Zribi, M., & Belhouchette, H. (2020, January). Irrigation Events Detection over Intensively Irrigated Grassland Plots Using Sentinel-1 Data. *Remote Sensing*, *12*(24), 4058. Retrieved 2021-10-20, from <https://www.mdpi.com/2072-4292/12/24/4058> (Number: 24 Publisher: Multidisciplinary Digital Publishing Institute) doi: 10.3390/rs12244058
- Bazzi, H., Baghdadi, N., Fayad, I., Zribi, M., Belhouchette, H., & Demarez, V. (2020, January). Near Real-Time Irrigation Detection at Plot Scale Using Sentinel-1 Data. *Remote Sensing*, *12*(9), 1456. Retrieved 2021-10-20, from <https://www.mdpi.com/2072-4292/12/9/1456> (Number: 9 Publisher: Multidisciplinary Digital Publishing Institute) doi: 10.3390/rs12091456
- Bonfils, C., & Lobell, D. (2007, August). Empirical evidence for a recent slowdown in irrigation-induced cooling. *Proceedings of the National Academy of Sciences*, *104*(34), 13582–13587. Retrieved 2021-10-11, from <https://www.pnas.org/content/104/34/13582> (Publisher: National Academy of Sciences Section: Physical Sciences) doi: 10.1073/pnas.0700144104
- Bretreger, D., Yeo, I.-Y., & Hancock, G. (2022, February). Quantifying irrigation water use with remote sensing: Soil water deficit modelling with uncertain soil parameters. *Agricultural Water Management*, *260*, 107299. Retrieved 2022-11-08, from <https://www.sciencedirect.com/science/article/pii/S037837742100576X> doi: 10.1016/j.agwat.2021.107299
- Brocca, L., Ciabatta, L., Massari, C., Moramarco, T., Hahn, S., Hasenauer, S., ... Levizzani, V. (2014). Soil as a natural rain gauge: Estimating global rainfall from satellite soil moisture data. *Journal of Geophysical Research: Atmospheres*, *119*(9), 5128–5141. Retrieved 2022-11-07, from <https://onlinelibrary.wiley.com/doi/abs/10.1002/2014JD021489> (.eprint: <https://onlinelibrary.wiley.com/doi/pdf/10.1002/2014JD021489>) doi: 10.1002/2014JD021489
- Brocca, L., Tarpanelli, A., Filippucci, P., Dorigo, W., Zaussinger, F., Gruber, A., &

- 732 Fernández-Prieto, D. (2018, December). How much water is used for irrigation?  
 733 A new approach exploiting coarse resolution satellite soil moisture products. *Internation-*  
 734 *al Journal of Applied Earth Observation and Geoinformation*, *73*, 752–766. Re-  
 735 trieved 2022-11-04, from [https://www.sciencedirect.com/science/article/pii/](https://www.sciencedirect.com/science/article/pii/S0303243418304793)  
 736 [S0303243418304793](https://www.sciencedirect.com/science/article/pii/S0303243418304793) doi: 10.1016/j.jag.2018.08.023
- 737 Brombacher, J., Silva, I. R. d. O., Degen, J., & Pelgrum, H. (2022, June). A  
 738 novel evapotranspiration based irrigation quantification method using the hydrolog-  
 739 ical similar pixels algorithm. *Agricultural Water Management*, *267*, 107602. Re-  
 740 trieved 2022-11-07, from [https://www.sciencedirect.com/science/article/pii/](https://www.sciencedirect.com/science/article/pii/S0378377422001494)  
 741 [S0378377422001494](https://www.sciencedirect.com/science/article/pii/S0378377422001494) doi: 10.1016/j.agwat.2022.107602
- 742 Busschaert, L., de Roos, S., Thiery, W., Raes, D., & De Lannoy, G. J. M. (2022, July). Net  
 743 irrigation requirement under different climate scenarios using AquaCrop over Europe.  
 744 *Hydrology and Earth System Sciences*, *26*(14), 3731–3752. Retrieved 2022-10-27, from  
 745 <https://hess.copernicus.org/articles/26/3731/2022/> (Publisher: Copernicus  
 746 GmbH) doi: 10.5194/hess-26-3731-2022
- 747 Cook, B. I., Shukla, S. P., Puma, M. J., & Nazarenko, L. S. (2015, March). Irrigation as an  
 748 historical climate forcing. *Climate Dynamics*, *44*(5), 1715–1730. Retrieved 2021-11-  
 749 19, from <https://doi.org/10.1007/s00382-014-2204-7> doi: 10.1007/s00382-014-  
 750 -2204-7
- 751 Dari, J., Brocca, L., Modanesi, S., Massari, C., Tarpanelli, A., Barbetta, S., ... Volden, E.  
 752 (in review). Regional data sets of high-resolution (1 and 6 km) irrigation estimates  
 753 from space. *Earth System Science Data Discussions*, 1–34. Retrieved 2023-01-23, from  
 754 <https://essd.copernicus.org/preprints/essd-2022-403/> (Publisher: Copernicus  
 755 GmbH) doi: 10.5194/essd-2022-403
- 756 Dari, J., Brocca, L., Quintana-Seguí, P., Escorihuela, M. J., Stefan, V., & Morbidelli, R.  
 757 (2020, January). Exploiting High-Resolution Remote Sensing Soil Moisture to Es-  
 758 timate Irrigation Water Amounts over a Mediterranean Region. *Remote Sensing*,  
 759 *12*(16), 2593. Retrieved 2021-10-20, from [https://www.mdpi.com/2072-4292/12/](https://www.mdpi.com/2072-4292/12/16/2593)  
 760 [16/2593](https://www.mdpi.com/2072-4292/12/16/2593) (Number: 16 Publisher: Multidisciplinary Digital Publishing Institute) doi:  
 761 10.3390/rs12162593
- 762 Das, N. N., Entekhabi, D., Dunbar, R. S., Chaubell, M. J., Colliander, A., Yueh, S., ...  
 763 Thibeault, M. (2019, November). The SMAP and Copernicus Sentinel 1A/B mi-  
 764 crowave active-passive high resolution surface soil moisture product. *Remote Sensing of*  
 765 *Environment*, *233*, 111380. Retrieved 2022-11-23, from [https://www.sciencedirect](https://www.sciencedirect.com/science/article/pii/S0034425719303992)  
 766 [.com/science/article/pii/S0034425719303992](https://www.sciencedirect.com/science/article/pii/S0034425719303992) doi: 10.1016/j.rse.2019.111380
- 767 Das, N. N., Jalilvand, E., Abolafia-Rosenzweig, R., Tajrishy, M., Kumar, S., & Moham-  
 768 madi, M. R. (in review). Is it Possible to Quantify Irrigation Water-Use by Assim-  
 769 ilating a High-Resolution Soil Moisture Product? *Authorea*. Retrieved 2022-11-07,  
 770 from <https://essopenarchive.org/doi/full/10.1002/essoar.10512082.1> doi:  
 771 10.1002/essoar.10512082.1
- 772 Davidson, M. W. J., & Furnell, R. (2021, July). ROSE-L: Copernicus L-Band Sar Mission.  
 773 In *2021 IEEE International Geoscience and Remote Sensing Symposium IGARSS* (pp.  
 774 872–873). (ISSN: 2153-7003) doi: 10.1109/IGARSS47720.2021.9554018
- 775 Dee, D. P., Rukhovets, L., Todling, R., da Silva, A. M., & Larson, J. W. (2001).  
 776 An adaptive buddy check for observational quality control. *Quarterly Journal of*  
 777 *the Royal Meteorological Society*, *127*(577), 2451–2471. Retrieved 2022-11-23, from  
 778 <https://onlinelibrary.wiley.com/doi/abs/10.1002/qj.49712757714> (eprint:  
 779 <https://onlinelibrary.wiley.com/doi/pdf/10.1002/qj.49712757714>) doi: 10.1002/qj  
 780 .49712757714
- 781 De Lannoy, G. J. M., Bechtold, M., Albergel, C., Brocca, L., Calvet, J.-C., Carrassi,  
 782 A., ... Steele-Dunne, S. (2022). Perspective on satellite-based land data assim-  
 783 ilation to estimate water cycle components in an era of advanced data availabil-  
 784 ity and model sophistication. *Frontiers in Water*, *4*. Retrieved 2022-11-03, from  
 785 <https://www.frontiersin.org/articles/10.3389/frwa.2022.981745>
- 786 de Roos, S., Busschaert, L., Lievens, H., Bechtold, M., & De Lannoy, G. J. M. (in review).

- 787 Optimisation and uncertainty assessment of AquaCrop backscatter simulations using  
788 Sentinel-1 observations. *Remote Sensing of Environment*.
- 789 Droogers, P., Immerzeel, W. W., & Lorite, I. J. (2010, September). Estimating actual  
790 irrigation application by remotely sensed evapotranspiration observations. *Agricultural Water Management*, *97*(9), 1351–1359. Retrieved 2022-11-08, from <https://www.sciencedirect.com/science/article/pii/S0378377410001149> doi: 10.1016/j.agwat.2010.03.017
- 793
- 794 Döll, P. (2002, August). Impact of Climate Change and Variability on Irrigation Requirements: A Global Perspective. *Climatic Change*, *54*(3), 269–293. Retrieved 2021-09-28, from <https://doi.org/10.1023/A:1016124032231> doi: 10.1023/A:1016124032231
- 795
- 796
- 797 Fischer, G., Tubiello, F. N., van Velthuizen, H., & Wiberg, D. A. (2007, September). Climate change impacts on irrigation water requirements: Effects of mitigation, 1990–2080. *Technological Forecasting and Social Change*, *74*(7), 1083–1107. Retrieved 2021-10-01, from <https://www.sciencedirect.com/science/article/pii/S0040162506001429> doi: 10.1016/j.techfore.2006.05.021
- 800
- 801
- 802 Foley, J. A., Ramankutty, N., Brauman, K. A., Cassidy, E. S., Gerber, J. S., Johnston, M., ... Zaks, D. P. M. (2011, October). Solutions for a cultivated planet. *Nature*, *478*(7369), 337–342. Retrieved 2022-11-03, from <https://www.nature.com/articles/nature10452> (Number: 7369 Publisher: Nature Publishing Group) doi: 10.1038/nature10452
- 803
- 804
- 805
- 806
- 807 Gelaro, R., McCarty, W., Suárez, M. J., Todling, R., Molod, A., Takacs, L., ... Zhao, B. (2017, July). The Modern-Era Retrospective Analysis for Research and Applications, Version 2 (MERRA-2). *Journal of Climate*, *30*(14), 5419–5454. Retrieved 2022-02-04, from <https://journals.ametsoc.org/view/journals/clim/30/14/jcli-d-16-0758.1.xml> (Publisher: American Meteorological Society Section: Journal of Climate) doi: 10.1175/JCLI-D-16-0758.1
- 808
- 809
- 810
- 811
- 812
- 813 Giroto, M., Reichle, R., Rodell, M., & Maggioni, V. (2021, January). Data Assimilation of Terrestrial Water Storage Observations to Estimate Precipitation Fluxes: A Synthetic Experiment. *Remote Sensing*, *13*(6), 1223. Retrieved 2022-05-16, from <https://www.mdpi.com/2072-4292/13/6/1223> (Number: 6 Publisher: Multidisciplinary Digital Publishing Institute) doi: 10.3390/rs13061223
- 814
- 815
- 816
- 817
- 818 Gleick, P. H., Cooley, H., Morikawa, M., Morrison, J., & Cohen, M. J. (2009). *The World's Water 2008-2009: The Biennial Report on Freshwater Resources*. Island Press. (Google-Books-ID: lyG8BwAAQBAJ)
- 819
- 820
- 821 Gormley-Gallagher, A. M., Sterl, S., Hirsch, A. L., Seneviratne, S. I., Davin, E. L., & Thiery, W. (2022, February). Agricultural management effects on mean and extreme temperature trends. *Earth System Dynamics*, *13*(1), 419–438. Retrieved 2022-11-08, from <https://esd.copernicus.org/articles/13/419/2022/> (Publisher: Copernicus GmbH) doi: 10.5194/esd-13-419-2022
- 822
- 823
- 824
- 825
- 826 Gutman, G., & Ignatov, A. (1998, January). The derivation of the green vegetation fraction from NOAA/AVHRR data for use in numerical weather prediction models. *International Journal of Remote Sensing*, *19*(8), 1533–1543. Retrieved 2022-11-16, from <https://doi.org/10.1080/014311698215333> (Publisher: Taylor & Francis .eprint: <https://doi.org/10.1080/014311698215333>) doi: 10.1080/014311698215333
- 827
- 828
- 829
- 830
- 831 Hersbach, H., Bell, B., Berrisford, P., Hirahara, S., Horányi, A., Muñoz-Sabater, J., ... Thépaut, J.-N. (2020). The ERA5 global reanalysis. *Quarterly Journal of the Royal Meteorological Society*, *146*(730), 1999–2049. Retrieved 2022-11-24, from <https://onlinelibrary.wiley.com/doi/abs/10.1002/qj.3803> (.eprint: <https://onlinelibrary.wiley.com/doi/pdf/10.1002/qj.3803>) doi: 10.1002/qj.3803
- 832
- 833
- 834
- 835
- 836 Hirsch, A. L., Wilhelm, M., Davin, E. L., Thiery, W., & Seneviratne, S. I. (2017). Can climate-effective land management reduce regional warming? *Journal of Geophysical Research: Atmospheres*, *122*(4), 2269–2288. Retrieved 2022-11-03, from <https://onlinelibrary.wiley.com/doi/abs/10.1002/2016JD026125> (.eprint: <https://onlinelibrary.wiley.com/doi/pdf/10.1002/2016JD026125>) doi: 10.1002/2016JD026125
- 837
- 838
- 839
- 840
- 841

- 842 Jalilvand, E., Tajrishy, M., Ghazi Zadeh Hashemi, S. A., & Brocca, L. (2019,  
843 September). Quantification of irrigation water using remote sensing of soil mois-  
844 ture in a semi-arid region. *Remote Sensing of Environment*, *231*, 111226. Re-  
845 trieved 2022-04-26, from [https://www.sciencedirect.com/science/article/pii/](https://www.sciencedirect.com/science/article/pii/S0034425719302457)  
846 [S0034425719302457](https://www.sciencedirect.com/science/article/pii/S0034425719302457) doi: 10.1016/j.rse.2019.111226
- 847 Jin, N., Tao, B., Ren, W., Feng, M., Sun, R., He, L., ... Yu, Q. (2016, March). Mapping  
848 Irrigated and Rainfed Wheat Areas Using Multi-Temporal Satellite Data. *Remote*  
849 *Sensing*, *8*(3), 207. Retrieved 2022-11-04, from [https://www.mdpi.com/2072-4292/](https://www.mdpi.com/2072-4292/8/3/207)  
850 [8/3/207](https://www.mdpi.com/2072-4292/8/3/207) (Number: 3 Publisher: Multidisciplinary Digital Publishing Institute) doi:  
851 10.3390/rs8030207
- 852 Kumar, S. V., Peters-Lidard, C. D., Santanello, J. A., Reichle, R. H., Draper, C. S., Koster,  
853 R. D., ... Jasinski, M. F. (2015, November). Evaluating the utility of satellite soil  
854 moisture retrievals over irrigated areas and the ability of land data assimilation meth-  
855 ods to correct for unmodeled processes. *Hydrology and Earth System Sciences*, *19*(11),  
856 4463–4478. Retrieved 2022-05-03, from [https://hess.copernicus.org/articles/](https://hess.copernicus.org/articles/19/4463/2015/)  
857 [19/4463/2015/](https://hess.copernicus.org/articles/19/4463/2015/) (Publisher: Copernicus GmbH) doi: 10.5194/hess-19-4463-2015
- 858 Kumar, S. V., Peters-Lidard, C. D., Tian, Y., Houser, P. R., Geiger, J., Olden, S., ...  
859 Sheffield, J. (2006, October). Land information system: An interoperable frame-  
860 work for high resolution land surface modeling. *Environmental Modelling & Software*,  
861 *21*(10), 1402–1415. Retrieved 2022-11-09, from [https://www.sciencedirect.com/](https://www.sciencedirect.com/science/article/pii/S1364815205001283)  
862 [science/article/pii/S1364815205001283](https://www.sciencedirect.com/science/article/pii/S1364815205001283) doi: 10.1016/j.envsoft.2005.07.004
- 863 Kumar, S. V., Reichle, R. H., Peters-Lidard, C. D., Koster, R. D., Zhan, X., Crow, W. T., ...  
864 Houser, P. R. (2008, November). A land surface data assimilation framework using the  
865 land information system: Description and applications. *Advances in Water Resources*,  
866 *31*(11), 1419–1432. Retrieved 2022-11-09, from [https://www.sciencedirect.com/](https://www.sciencedirect.com/science/article/pii/S0309170808000146)  
867 [science/article/pii/S0309170808000146](https://www.sciencedirect.com/science/article/pii/S0309170808000146) doi: 10.1016/j.advwatres.2008.01.013
- 868 Kwon, Y., Kumar, S. V., Navari, M., Mocko, D. M., Kemp, E. M., Wegiel, J. W., ...  
869 Bindlish, R. (2022, July). Irrigation characterization improved by the direct use  
870 of SMAP soil moisture anomalies within a data assimilation system. *Environmental*  
871 *Research Letters*, *17*(8), 084006. Retrieved 2022-09-21, from [https://doi.org/10](https://doi.org/10.1088/1748-9326/ac7f49)  
872 [.1088/1748-9326/ac7f49](https://doi.org/10.1088/1748-9326/ac7f49) (Publisher: IOP Publishing) doi: 10.1088/1748-9326/  
873 [ac7f49](https://doi.org/10.1088/1748-9326/ac7f49)
- 874 Le Page, M., Berjamy, B., Fakir, Y., Bourgin, F., Jarlan, L., Abourida, A., ... Chehbouni,  
875 G. (2012, September). An Integrated DSS for Groundwater Management Based  
876 on Remote Sensing. The Case of a Semi-arid Aquifer in Morocco. *Water Resources*  
877 *Management*, *26*(11), 3209–3230. Retrieved 2022-11-08, from [https://doi.org/10](https://doi.org/10.1007/s11269-012-0068-3)  
878 [.1007/s11269-012-0068-3](https://doi.org/10.1007/s11269-012-0068-3) doi: 10.1007/s11269-012-0068-3
- 879 Magidi, J., Nhamo, L., Mpandeli, S., & Mabhaudhi, T. (2021, January). Application of the  
880 Random Forest Classifier to Map Irrigated Areas Using Google Earth Engine. *Remote*  
881 *Sensing*, *13*(5), 876. Retrieved 2022-11-04, from [https://www.mdpi.com/2072-4292/](https://www.mdpi.com/2072-4292/13/5/876)  
882 [13/5/876](https://www.mdpi.com/2072-4292/13/5/876) (Number: 5 Publisher: Multidisciplinary Digital Publishing Institute) doi:  
883 10.3390/rs13050876
- 884 Mahmood, R., Pielke Sr., R. A., Hubbard, K. G., Niyogi, D., Dirmeyer, P. A., McAlpine,  
885 C., ... Fall, S. (2014). Land cover changes and their biogeophysical effects on cli-  
886 mate. *International Journal of Climatology*, *34*(4), 929–953. Retrieved 2021-10-18,  
887 from <https://onlinelibrary.wiley.com/doi/abs/10.1002/joc.3736> (eprint:  
888 <https://onlinelibrary.wiley.com/doi/pdf/10.1002/joc.3736>) doi: 10.1002/joc.3736
- 889 Malbêteau, Y., Merlin, O., Molero, B., Rüdiger, C., & Bacon, S. (2016, March). Dis-  
890 PATCH as a tool to evaluate coarse-scale remotely sensed soil moisture using localized  
891 in situ measurements: Application to SMOS and AMSR-E data in Southeastern Aus-  
892 tralia. *International Journal of Applied Earth Observation and Geoinformation*, *45*,  
893 221–234. Retrieved 2022-12-06, from [https://www.sciencedirect.com/science/](https://www.sciencedirect.com/science/article/pii/S0303243415300386)  
894 [article/pii/S0303243415300386](https://www.sciencedirect.com/science/article/pii/S0303243415300386) doi: 10.1016/j.jag.2015.10.002
- 895 Maselli, F., Battista, P., Chiesi, M., Rapi, B., Angeli, L., Fibbi, L., ... Gozzini, B.  
896 (2020, December). Use of Sentinel-2 MSI data to monitor crop irrigation in Mediter-

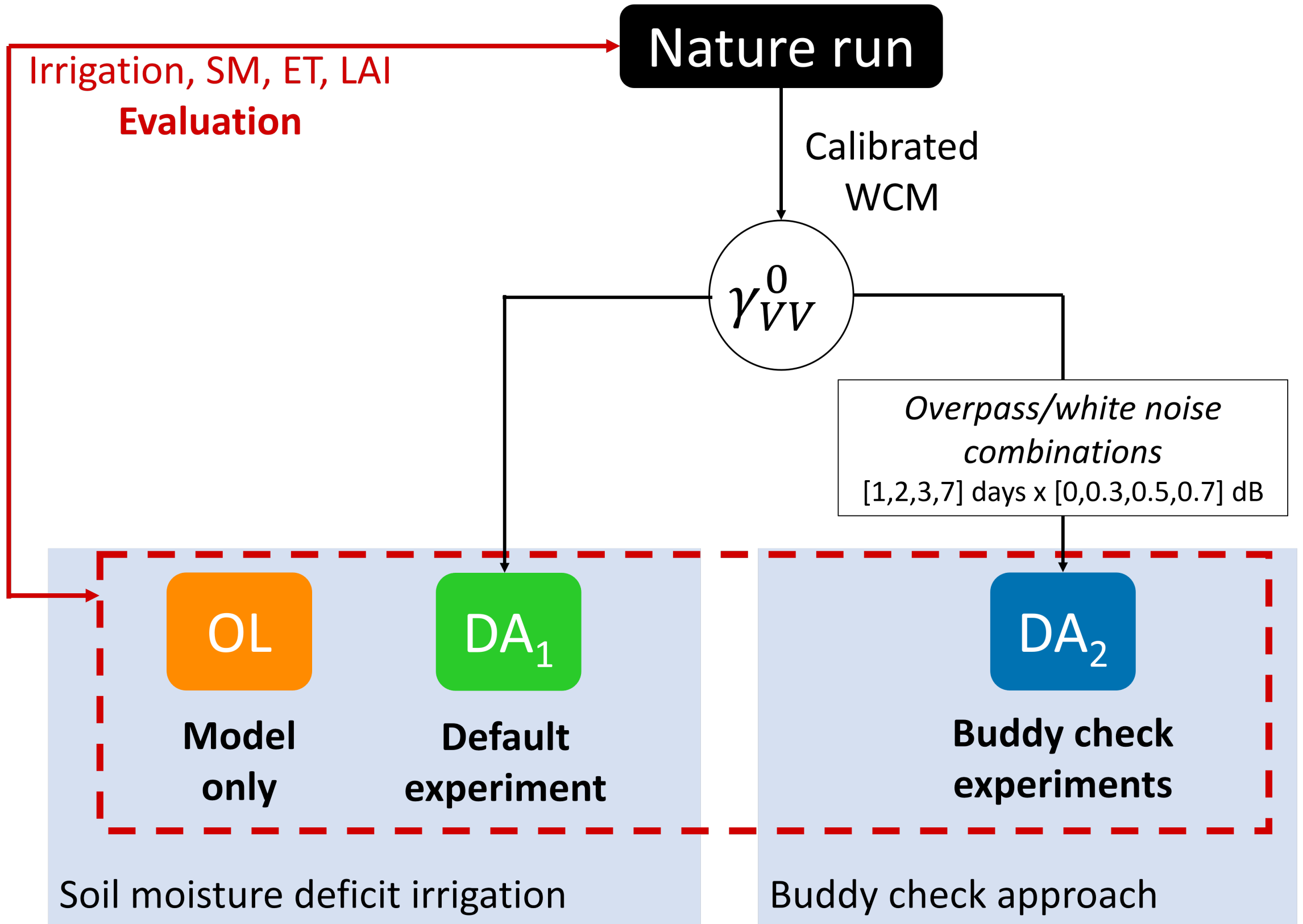
- 897 ranean areas. *International Journal of Applied Earth Observation and Geoinforma-*  
 898 *tion*, 93, 102216. Retrieved 2022-11-04, from [https://www.sciencedirect.com/](https://www.sciencedirect.com/science/article/pii/S0303243420302531)  
 899 [science/article/pii/S0303243420302531](https://www.sciencedirect.com/science/article/pii/S0303243420302531) doi: 10.1016/j.jag.2020.102216
- 900 Massari, C., Modanesi, S., Dari, J., Gruber, A., De Lannoy, G. J. M., Giroto, M., ...  
 901 Brocca, L. (2021, January). A Review of Irrigation Information Retrievals from  
 902 Space and Their Utility for Users. *Remote Sensing*, 13(20), 4112. Retrieved 2021-10-  
 903 20, from <https://www.mdpi.com/2072-4292/13/20/4112> (Number: 20 Publisher:  
 904 Multidisciplinary Digital Publishing Institute) doi: 10.3390/rs13204112
- 905 McNairn, H., & Shang, J. (2016). A Review of Multitemporal Synthetic Aperture Radar  
 906 (SAR) for Crop Monitoring. In Y. Ban (Ed.), *Multitemporal Remote Sensing: Methods*  
 907 *and Applications* (pp. 317–340). Cham: Springer International Publishing. Retrieved  
 908 2023-01-23, from [https://doi.org/10.1007/978-3-319-47037-5\\_15](https://doi.org/10.1007/978-3-319-47037-5_15) doi: 10.1007/  
 909 978-3-319-47037-5\_15
- 910 Merlin, O., Chehbouni, A., Walker, J. P., Panciera, R., & Kerr, Y. H. (2008, March).  
 911 A Simple Method to Disaggregate Passive Microwave-Based Soil Moisture. *IEEE*  
 912 *Transactions on Geoscience and Remote Sensing*, 46(3), 786–796. (Conference Name:  
 913 IEEE Transactions on Geoscience and Remote Sensing) doi: 10.1109/TGRS.2007  
 914 .914807
- 915 Miranda, N., Meadows, P., Piantanida, R., Recchia, A., Small, D., Schubert, A., ... Vega,  
 916 F. C. (2017, July). The Sentinel-1 constellation mission performance. In *2017 IEEE*  
 917 *International Geoscience and Remote Sensing Symposium (IGARSS)* (pp. 5541–5544).  
 918 (ISSN: 2153-7003) doi: 10.1109/IGARSS.2017.8128259
- 919 Modanesi, S., Massari, C., Bechtold, M., Lievens, H., Tarpanelli, A., Brocca, L., ... De Lan-  
 920 noy, G. J. M. (2022, September). Challenges and benefits of quantifying irrigation  
 921 through the assimilation of Sentinel-1 backscatter observations into Noah-MP. *Hy-*  
 922 *drology and Earth System Sciences*, 26(18), 4685–4706. Retrieved 2022-10-27, from  
 923 <https://hess.copernicus.org/articles/26/4685/2022/> (Publisher: Copernicus  
 924 GmbH) doi: 10.5194/hess-26-4685-2022
- 925 Modanesi, S., Massari, C., Gruber, A., Lievens, H., Tarpanelli, A., Morbidelli, R., &  
 926 De Lannoy, G. J. M. (2021, June). Optimizing a backscatter forward operator us-  
 927 ing Sentinel-1 data over irrigated land. *Hydrology and Earth System Sciences Discus-*  
 928 *sions*, 1–39. Retrieved 2021-10-20, from [https://hess.copernicus.org/preprints/](https://hess.copernicus.org/preprints/hess-2021-273/)  
 929 [hess-2021-273/](https://hess-2021-273/) (Publisher: Copernicus GmbH) doi: 10.5194/hess-2021-273
- 930 Nagaraj, D., Proust, E., Todeschini, A., Rulli, M. C., & D’Odorico, P. (2021, June).  
 931 A new dataset of global irrigation areas from 2001 to 2015. *Advances in Water Re-*  
 932 *sources*, 152, 103910. Retrieved 2022-11-03, from [https://www.sciencedirect.com/](https://www.sciencedirect.com/science/article/pii/S0309170821000658)  
 933 [science/article/pii/S0309170821000658](https://www.sciencedirect.com/science/article/pii/S0309170821000658) doi: 10.1016/j.advwatres.2021.103910
- 934 Nie, W., Kumar, S. V., Peters-Lidard, C. D., Zaitchik, B. F., Arsenault, K. R.,  
 935 Bindlish, R., & Liu, P.-W. (2022). Assimilation of Remotely Sensed Leaf Area  
 936 Index Enhances the Estimation of Anthropogenic Irrigation Water Use. *Journal*  
 937 *of Advances in Modeling Earth Systems*, 14(11), e2022MS003040. Retrieved 2022-  
 938 11-17, from <https://onlinelibrary.wiley.com/doi/abs/10.1029/2022MS003040>  
 939 (eprint: <https://onlinelibrary.wiley.com/doi/pdf/10.1029/2022MS003040>) doi: 10  
 940 .1029/2022MS003040
- 941 Niu, G.-Y., Yang, Z.-L., Mitchell, K. E., Chen, F., Ek, M. B., Barlage, M., ... Xia,  
 942 Y. (2011). The community Noah land surface model with multiparameterization  
 943 options (Noah-MP): 1. Model description and evaluation with local-scale measure-  
 944 ments. *Journal of Geophysical Research: Atmospheres*, 116(D12). Retrieved 2022-  
 945 02-08, from <https://onlinelibrary.wiley.com/doi/abs/10.1029/2010JD015139>  
 946 (eprint: <https://onlinelibrary.wiley.com/doi/pdf/10.1029/2010JD015139>) doi: 10  
 947 .1029/2010JD015139
- 948 Olivera-Guerra, L., Merlin, O., & Er-Raki, S. (2020, March). Irrigation retrieval from  
 949 Landsat optical/thermal data integrated into a crop water balance model: A case  
 950 study over winter wheat fields in a semi-arid region. *Remote Sensing of Environ-*  
 951 *ment*, 239, 111627. Retrieved 2022-11-08, from <https://www.sciencedirect.com/>

- 952 science/article/pii/S0034425719306479 doi: 10.1016/j.rse.2019.111627
- 953 Ouadi, N., Jarlan, L., Khabba, S., Ezzahar, J., Le Page, M., & Merlin, O. (2021, January).  
 954 Irrigation Amounts and Timing Retrieval through Data Assimilation of Surface Soil  
 955 Moisture into the FAO-56 Approach in the South Mediterranean Region. *Remote Sensing*,  
 956 *13*(14), 2667. Retrieved 2021-10-20, from [https://www.mdpi.com/2072-4292/](https://www.mdpi.com/2072-4292/13/14/2667)  
 957 [13/14/2667](https://www.mdpi.com/2072-4292/13/14/2667) (Number: 14 Publisher: Multidisciplinary Digital Publishing Institute)  
 958 doi: 10.3390/rs13142667
- 959 Ozdogan, M., & Gutman, G. (2008, September). A new methodology to map irri-  
 960 gated areas using multi-temporal MODIS and ancillary data: An application example  
 961 in the continental US. *Remote Sensing of Environment*, *112*(9), 3520–3537. Re-  
 962 trieved 2022-11-03, from [https://www.sciencedirect.com/science/article/pii/](https://www.sciencedirect.com/science/article/pii/S0034425708001338)  
 963 [S0034425708001338](https://www.sciencedirect.com/science/article/pii/S0034425708001338) doi: 10.1016/j.rse.2008.04.010
- 964 Ozdogan, M., Rodell, M., Beaudoin, H. K., & Toll, D. L. (2010, February). Simulat-  
 965 ing the Effects of Irrigation over the United States in a Land Surface Model Based  
 966 on Satellite-Derived Agricultural Data. *Journal of Hydrometeorology*, *11*(1), 171–  
 967 184. Retrieved 2022-11-07, from [https://journals.ametsoc.org/view/journals/](https://journals.ametsoc.org/view/journals/hydr/11/1/2009jhm1116.1.xml)  
 968 [hydr/11/1/2009jhm1116.1.xml](https://journals.ametsoc.org/view/journals/hydr/11/1/2009jhm1116.1.xml) (Publisher: American Meteorological Society Sec-  
 969 tion: Journal of Hydrometeorology) doi: 10.1175/2009JHM1116.1
- 970 Patel, P., Srivastava, H. S., Panigrahy, S., & Parihar, J. S. (2006, January). Compara-  
 971 tive evaluation of the sensitivity of multi-polarized multi-frequency SAR backscatter  
 972 to plant density. *International Journal of Remote Sensing*, *27*(2), 293–305. Re-  
 973 trieved 2022-12-06, from <https://doi.org/10.1080/01431160500214050> (Pub-  
 974 lisher: Taylor & Francis eprint: <https://doi.org/10.1080/01431160500214050>) doi:  
 975 10.1080/01431160500214050
- 976 Pervez, S., Budde, M., & Rowland, J. (2014, June). Mapping irrigated areas in Afghanistan  
 977 over the past decade using MODIS NDVI. *Remote Sensing of Environment*, *149*,  
 978 155–165. Retrieved 2022-11-04, from [https://www.sciencedirect.com/science/](https://www.sciencedirect.com/science/article/pii/S0034425714001461)  
 979 [article/pii/S0034425714001461](https://www.sciencedirect.com/science/article/pii/S0034425714001461) doi: 10.1016/j.rse.2014.04.008
- 980 Rains, D., Lievens, H., De Lannoy, G. J. M., McCabe, M. F., de Jeu, R. A. M., & Miralles,  
 981 D. G. (2022). Sentinel-1 Backscatter Assimilation Using Support Vector Regression  
 982 or the Water Cloud Model at European Soil Moisture Sites. *IEEE Geoscience and*  
 983 *Remote Sensing Letters*, *19*, 1–5. (Conference Name: IEEE Geoscience and Remote  
 984 Sensing Letters) doi: 10.1109/LGRS.2021.3073484
- 985 Rodríguez-Fernández, N. J., Anterrieu, E., Rougé, B., Boutin, J., Picard, G., Pellarin, T., . . .  
 986 Kerr, Y. H. (2019, July). SMOS-HR: A High Resolution L-Band Passive Radiometer  
 987 for Earth Science and Applications. In *IGARSS 2019 - 2019 IEEE International*  
 988 *Geoscience and Remote Sensing Symposium* (pp. 8392–8395). (ISSN: 2153-7003) doi:  
 989 10.1109/IGARSS.2019.8897815
- 990 Roebber, P. J. (2009, April). Visualizing Multiple Measures of Forecast Quality.  
 991 *Weather and Forecasting*, *24*(2), 601–608. Retrieved 2022-08-25, from [https://](https://journals.ametsoc.org/view/journals/wefo/24/2/2008waf2222159.1.xml)  
 992 [journals.ametsoc.org/view/journals/wefo/24/2/2008waf2222159.1.xml](https://journals.ametsoc.org/view/journals/wefo/24/2/2008waf2222159.1.xml) (Pub-  
 993 lisher: American Meteorological Society Section: Weather and Forecasting) doi:  
 994 10.1175/2008WAF2222159.1
- 995 Ryu, D., Crow, W. T., Zhan, X., & Jackson, T. J. (2009, June). Correcting Unintended  
 996 Perturbation Biases in Hydrologic Data Assimilation. *Journal of Hydrometeorology*,  
 997 *10*(3), 734–750. Retrieved 2022-11-09, from [https://journals.ametsoc.org/view/](https://journals.ametsoc.org/view/journals/hydr/10/3/2008jhm1038.1.xml)  
 998 [journals/hydr/10/3/2008jhm1038.1.xml](https://journals.ametsoc.org/view/journals/hydr/10/3/2008jhm1038.1.xml) (Publisher: American Meteorological So-  
 999 ciety Section: Journal of Hydrometeorology) doi: 10.1175/2008JHM1038.1
- 1000 Salmon, J. M., Friedl, M. A., Frolking, S., Wisser, D., & Douglas, E. M. (2015,  
 1001 June). Global rain-fed, irrigated, and paddy croplands: A new high resolution  
 1002 map derived from remote sensing, crop inventories and climate data. *Internation-*  
 1003 *al Journal of Applied Earth Observation and Geoinformation*, *38*, 321–334. Re-  
 1004 trieved 2021-10-20, from [https://www.sciencedirect.com/science/article/pii/](https://www.sciencedirect.com/science/article/pii/S0303243415000240)  
 1005 [S0303243415000240](https://www.sciencedirect.com/science/article/pii/S0303243415000240) doi: 10.1016/j.jag.2015.01.014
- 1006 Siebert, S., Kumm, M., Porkka, M., Döll, P., Ramankutty, N., & Scanlon, B. R. (2015,

- 1007 March). A global data set of the extent of irrigated land from 1900 to 2005. *Hydrology*  
 1008 *and Earth System Sciences*, 19(3), 1521–1545. Retrieved 2022-10-27, from [https://](https://hess.copernicus.org/articles/19/1521/2015/)  
 1009 [hess.copernicus.org/articles/19/1521/2015/](https://hess.copernicus.org/articles/19/1521/2015/) (Publisher: Copernicus GmbH)  
 1010 doi: 10.5194/hess-19-1521-2015
- 1011 Thiery, W., Davin, E. L., Lawrence, D. M., Hirsch, A. L., Hauser, M., & Senevi-  
 1012 ratne, S. I. (2017). Present-day irrigation mitigates heat extremes. *Journal of Geophysical Research: Atmospheres*, 122(3), 1403–1422. Retrieved 2021-  
 1013 10-18, from <https://onlinelibrary.wiley.com/doi/abs/10.1002/2016JD025740>  
 1014 (\_eprint: <https://onlinelibrary.wiley.com/doi/pdf/10.1002/2016JD025740>) doi: 10  
 1015 .1002/2016JD025740
- 1016 Thiery, W., Visser, A. J., Fischer, E. M., Hauser, M., Hirsch, A. L., Lawrence, D. M.,  
 1017 ... Seneviratne, S. I. (2020, January). Warming of hot extremes alleviated by ex-  
 1018 panding irrigation. *Nature Communications*, 11(1), 290. Retrieved 2021-09-29, from  
 1019 <https://www.nature.com/articles/s41467-019-14075-4> (Bandiera\_abtest: a  
 1020 Cc\_license\_type: cc.by Cg\_type: Nature Research Journals Number: 1 Primary\_atype:  
 1021 Research Publisher: Nature Publishing Group Subject\_term: Attribution;Climate and  
 1022 Earth system modelling;Hydrology Subject\_term\_id: attribution;climate-and-earth-  
 1023 system-modelling;hydrology) doi: 10.1038/s41467-019-14075-4
- 1024 Torres, R., Snoeij, P., Geudtner, D., Bibby, D., Davidson, M., Attema, E., ... Ros-  
 1025 tan, F. (2012, May). GMES Sentinel-1 mission. *Remote Sensing of Environment*,  
 1026 120, 9–24. Retrieved 2022-11-04, from [https://www.sciencedirect.com/science/](https://www.sciencedirect.com/science/article/pii/S0034425712000600)  
 1027 [article/pii/S0034425712000600](https://www.sciencedirect.com/science/article/pii/S0034425712000600) doi: 10.1016/j.rse.2011.05.028
- 1028 Valmassoi, A., & Keller, J. D. (2022). A review on irrigation parameterizations in Earth  
 1029 system models. *Frontiers in Water*, 4. Retrieved 2023-02-07, from [https://www](https://www.frontiersin.org/articles/10.3389/frwa.2022.906664)  
 1030 [.frontiersin.org/articles/10.3389/frwa.2022.906664](https://www.frontiersin.org/articles/10.3389/frwa.2022.906664)
- 1031 van Eekelen, M. W., Bastiaanssen, W. G. M., Jarmain, C., Jackson, B., Ferreira, F., van der  
 1032 Zaag, P., ... Luxemburg, W. M. J. (2015, February). A novel approach to estimate  
 1033 direct and indirect water withdrawals from satellite measurements: A case study from  
 1034 the Incomati basin. *Agriculture, Ecosystems & Environment*, 200, 126–142. Re-  
 1035 trieved 2022-11-08, from [https://www.sciencedirect.com/science/article/pii/](https://www.sciencedirect.com/science/article/pii/S0167880914004861)  
 1036 [S0167880914004861](https://www.sciencedirect.com/science/article/pii/S0167880914004861) doi: 10.1016/j.agee.2014.10.023
- 1037 van Leeuwen, P. J. (2015). Representation errors and retrievals in linear and nonlinear data  
 1038 assimilation. *Quarterly Journal of the Royal Meteorological Society*, 141(690), 1612–  
 1039 1623. Retrieved 2023-01-26, from [https://onlinelibrary.wiley.com/doi/abs/10](https://onlinelibrary.wiley.com/doi/abs/10.1002/qj.2464)  
 1040 [.1002/qj.2464](https://onlinelibrary.wiley.com/doi/abs/10.1002/qj.2464) (\_eprint: <https://onlinelibrary.wiley.com/doi/pdf/10.1002/qj.2464>)  
 1041 doi: 10.1002/qj.2464
- 1042 Vogels, M. F. A., de Jong, S. M., Sterk, G., Wanders, N., Bierkens, M. F. P., & Addink, E. A.  
 1043 (2020, June). An object-based image analysis approach to assess irrigation-water con-  
 1044 sumption from MODIS products in Ethiopia. *International Journal of Applied Earth*  
 1045 *Observation and Geoinformation*, 88, 102067. Retrieved 2022-11-04, from [https://](https://www.sciencedirect.com/science/article/pii/S0303243419311833)  
 1046 [www.sciencedirect.com/science/article/pii/S0303243419311833](https://www.sciencedirect.com/science/article/pii/S0303243419311833) doi: 10.1016/  
 1047 j.jag.2020.102067
- 1048 Vreugdenhil, M., Wagner, W., Bauer-Marschallinger, B., Pfeil, I., Teubner, I., Rüdiger, C.,  
 1049 & Strauss, P. (2018, September). Sensitivity of Sentinel-1 Backscatter to Vegetation  
 1050 Dynamics: An Austrian Case Study. *Remote Sensing*, 10(9), 1396. Retrieved 2022-  
 1051 12-06, from <https://www.mdpi.com/2072-4292/10/9/1396> (Number: 9 Publisher:  
 1052 Multidisciplinary Digital Publishing Institute) doi: 10.3390/rs10091396
- 1053 Xie, Y., & Lark, T. J. (2021, July). Mapping annual irrigation from Landsat imagery and  
 1054 environmental variables across the conterminous United States. *Remote Sensing of*  
 1055 *Environment*, 260, 112445. Retrieved 2022-11-04, from [https://www.sciencedirect](https://www.sciencedirect.com/science/article/pii/S0034425721001632)  
 1056 [.com/science/article/pii/S0034425721001632](https://www.sciencedirect.com/science/article/pii/S0034425721001632) doi: 10.1016/j.rse.2021.112445
- 1057 Zappa, L., Schlaffer, S., Bauer-Marschallinger, B., Nendel, C., Zimmerman, B., & Dorigo,  
 1058 W. (2021, January). Detection and Quantification of Irrigation Water Amounts at  
 1059 500 m Using Sentinel-1 Surface Soil Moisture. *Remote Sensing*, 13(9), 1727. Re-  
 1060 trieved 2021-10-20, from <https://www.mdpi.com/2072-4292/13/9/1727> (Number:  
 1061

- 1062 9 Publisher: Multidisciplinary Digital Publishing Institute) doi: 10.3390/rs13091727  
 1063 Zappa, L., Schlaffer, S., Brocca, L., Vreugdenhil, M., Nendel, C., & Dorigo, W. (2022,  
 1064 September). How accurately can we retrieve irrigation timing and water amounts  
 1065 from (satellite) soil moisture? *International Journal of Applied Earth Obser-*  
 1066 *vation and Geoinformation*, *113*, 102979. Retrieved 2022-08-24, from [https://](https://www.sciencedirect.com/science/article/pii/S1569843222001704)  
 1067 [www.sciencedirect.com/science/article/pii/S1569843222001704](https://www.sciencedirect.com/science/article/pii/S1569843222001704) doi: 10.1016/  
 1068 j.jag.2022.102979
- 1069 Zaussinger, F., Dorigo, W., Gruber, A., Tarpanelli, A., Filippucci, P., & Brocca, L. (2019,  
 1070 February). Estimating irrigation water use over the contiguous United States by  
 1071 combining satellite and reanalysis soil moisture data. *Hydrology and Earth System*  
 1072 *Sciences*, *23*(2), 897–923. Retrieved 2022-11-07, from [https://hess.copernicus](https://hess.copernicus.org/articles/23/897/2019/)  
 1073 [.org/articles/23/897/2019/](https://hess.copernicus.org/articles/23/897/2019/) (Publisher: Copernicus GmbH) doi: 10.5194/hess-23  
 1074 -897-2019
- 1075 Zhang, C., Dong, J., & Ge, Q. (2022, October). IrriMap.cn: Annual irrigation  
 1076 maps across China in 2000–2019 based on satellite observations, environmental vari-  
 1077 ables, and machine learning. *Remote Sensing of Environment*, *280*, 113184. Re-  
 1078 trieved 2022-08-02, from [https://www.sciencedirect.com/science/article/pii/](https://www.sciencedirect.com/science/article/pii/S0034425722002966)  
 1079 [S0034425722002966](https://www.sciencedirect.com/science/article/pii/S0034425722002966) doi: 10.1016/j.rse.2022.113184
- 1080 Zhang, L., Zhang, K., Zhu, X., Chen, H., & Wang, W. (2022, October). Integrat-  
 1081 ing remote sensing, irrigation suitability and statistical data for irrigated crop-  
 1082 land mapping over mainland China. *Journal of Hydrology*, *613*, 128413. Re-  
 1083 trieved 2022-11-04, from [https://www.sciencedirect.com/science/article/pii/](https://www.sciencedirect.com/science/article/pii/S0022169422009830)  
 1084 [S0022169422009830](https://www.sciencedirect.com/science/article/pii/S0022169422009830) doi: 10.1016/j.jhydrol.2022.128413
- 1085 Zohaib, M., & Choi, M. (2020, April). Satellite-based global-scale irrigation water use  
 1086 and its contemporary trends. *Science of The Total Environment*, *714*, 136719. Re-  
 1087 trieved 2022-11-07, from [https://www.sciencedirect.com/science/article/pii/](https://www.sciencedirect.com/science/article/pii/S0048969720302291)  
 1088 [S0048969720302291](https://www.sciencedirect.com/science/article/pii/S0048969720302291) doi: 10.1016/j.scitotenv.2020.136719

**Figure 1.**



**Nature run**

**Irrigation, SM, ET, LAI  
Evaluation**

Calibrated  
WCM

$\gamma_{VV}^0$

*Overpass/white noise  
combinations*

$[1,2,3,7] \text{ days} \times [0,0.3,0.5,0.7] \text{ dB}$

**OL**

**Model  
only**

**DA<sub>1</sub>**

**Default  
experiment**

**DA<sub>2</sub>**

**Buddy check  
experiments**

Soil moisture deficit irrigation

Buddy check approach

Figure 2.

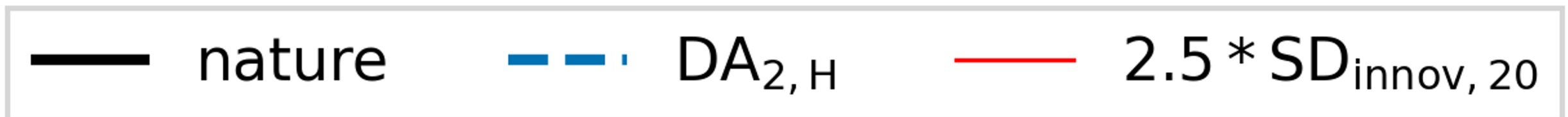
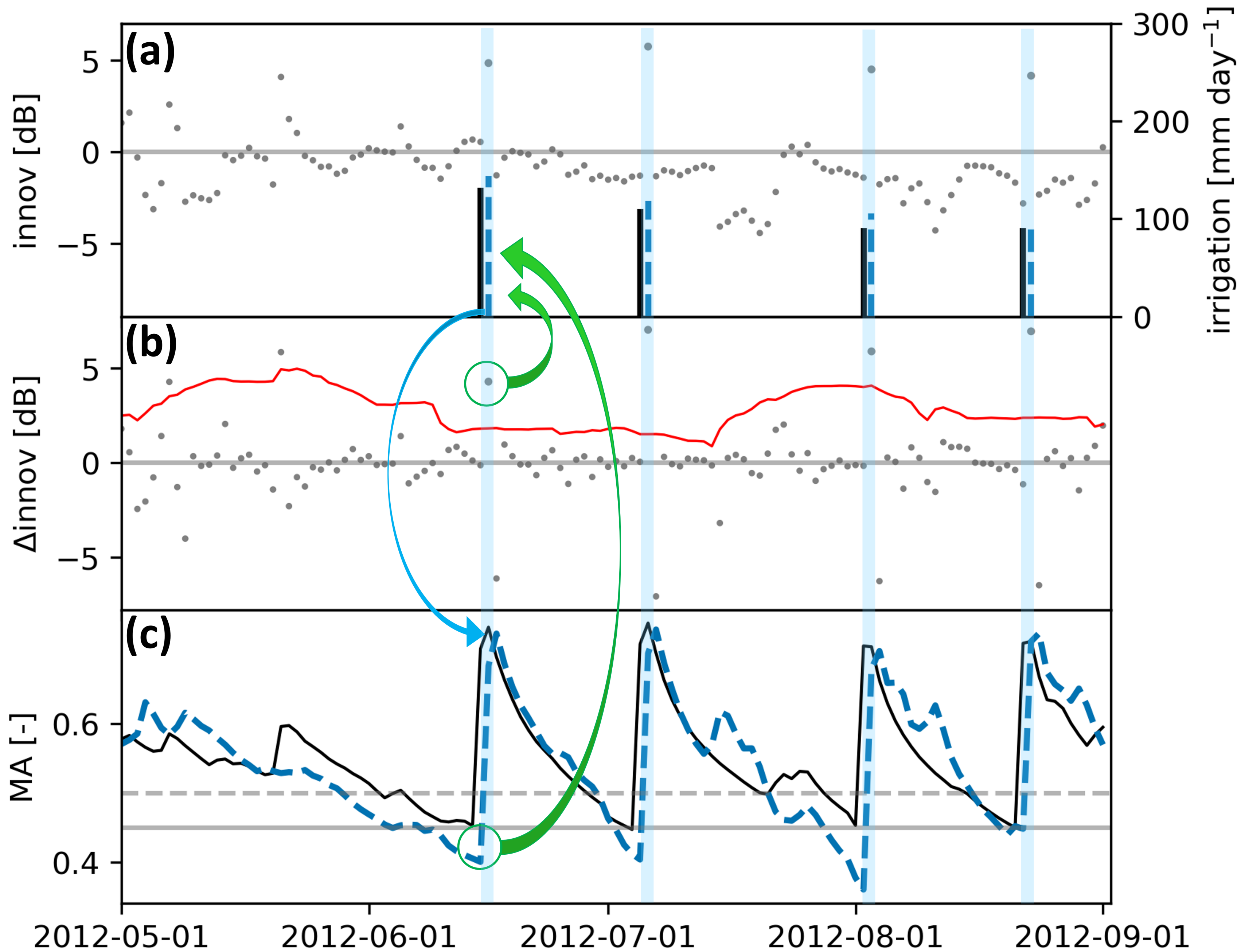


Figure 3.

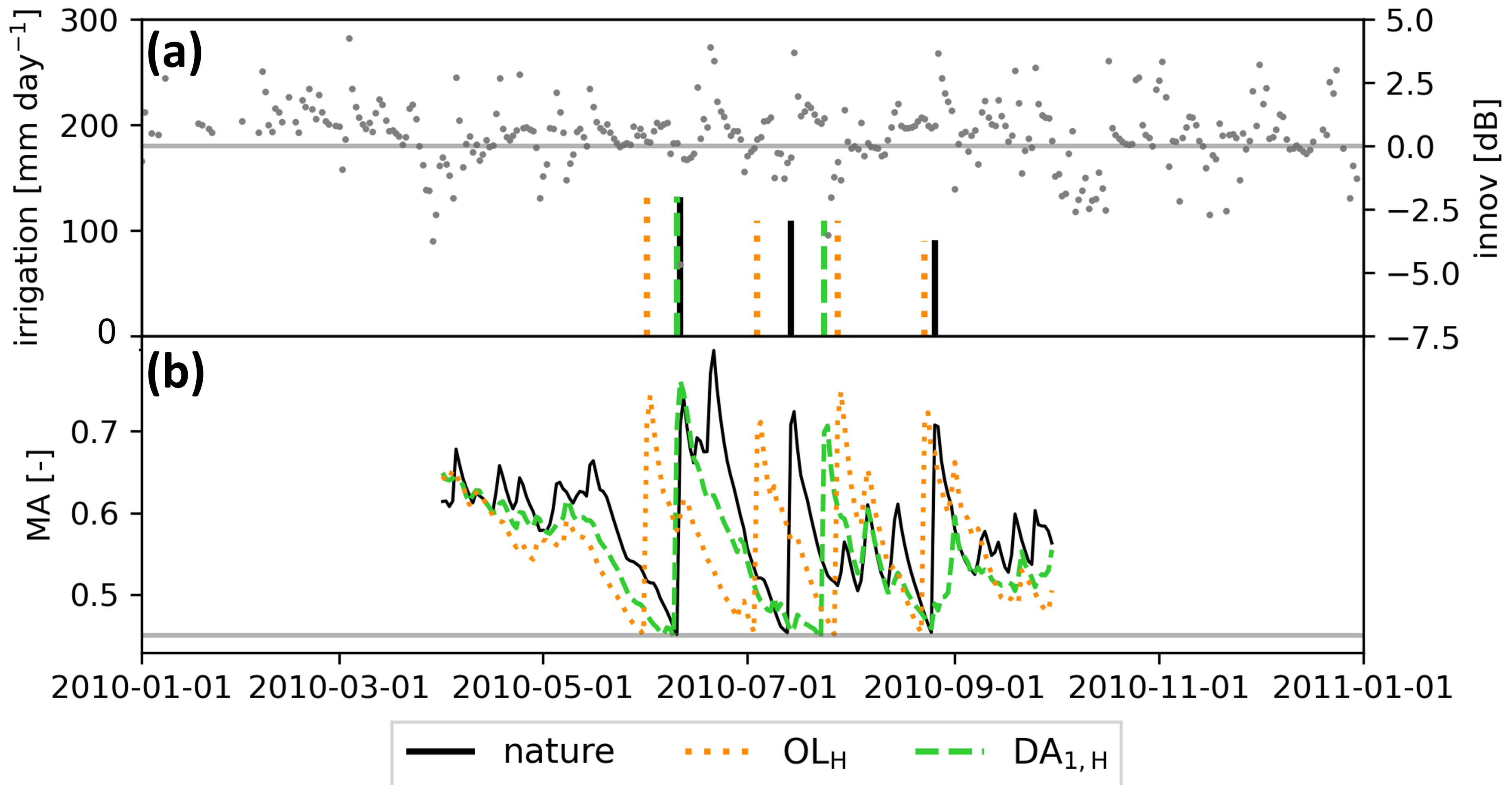


Figure 4.

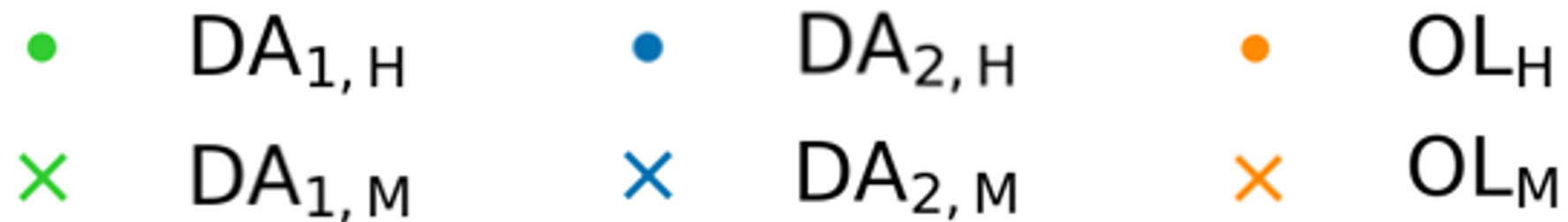
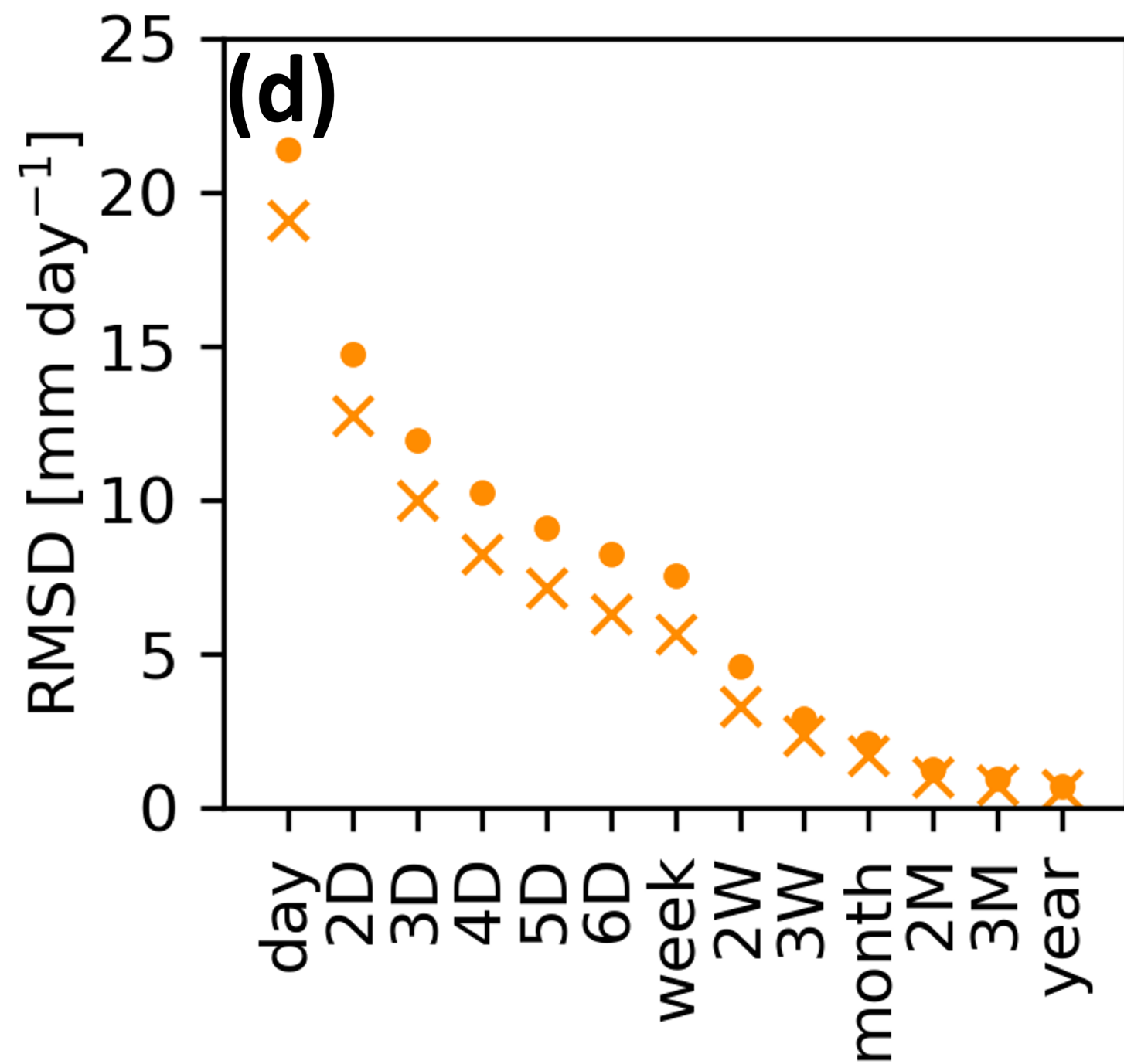
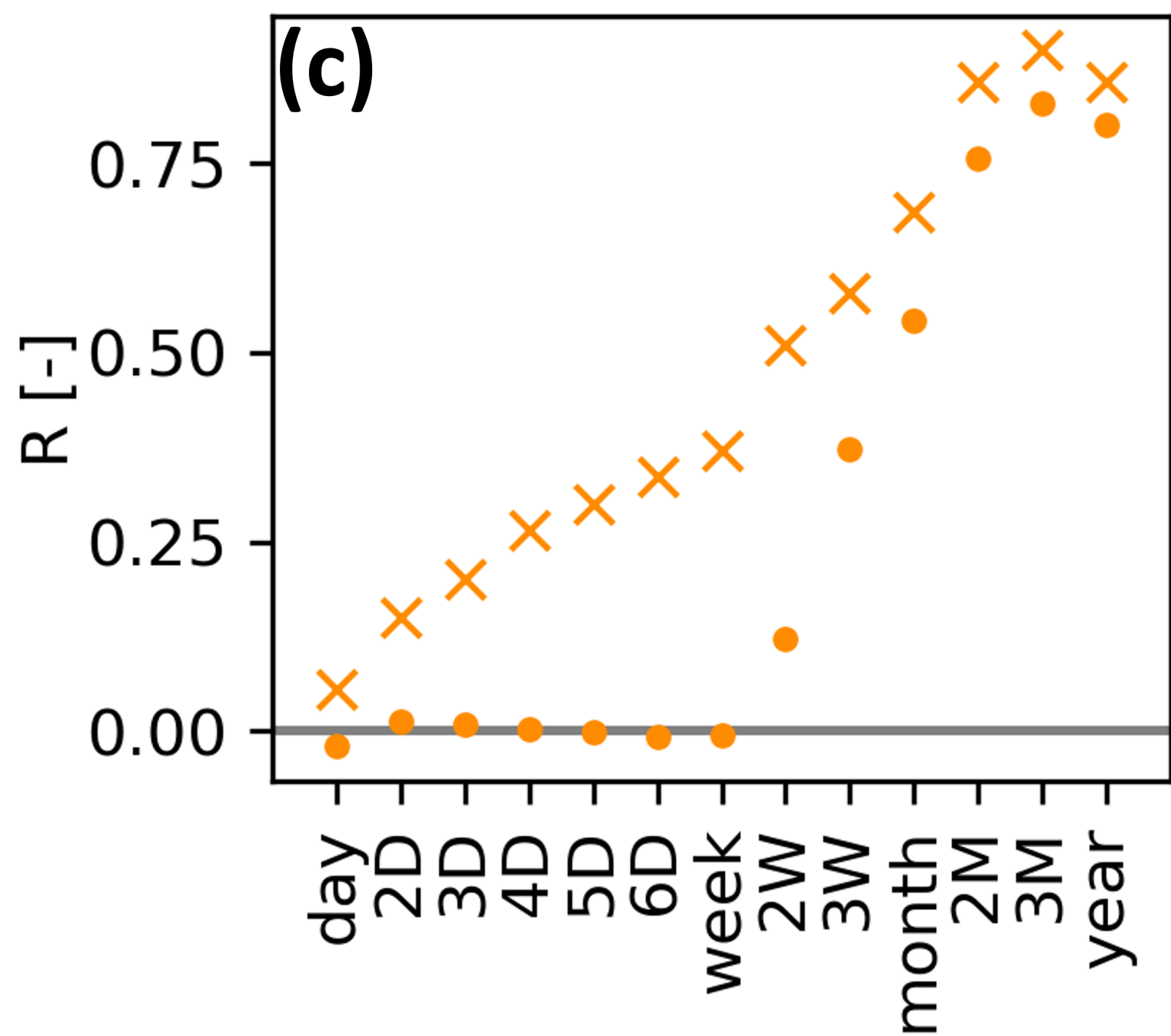
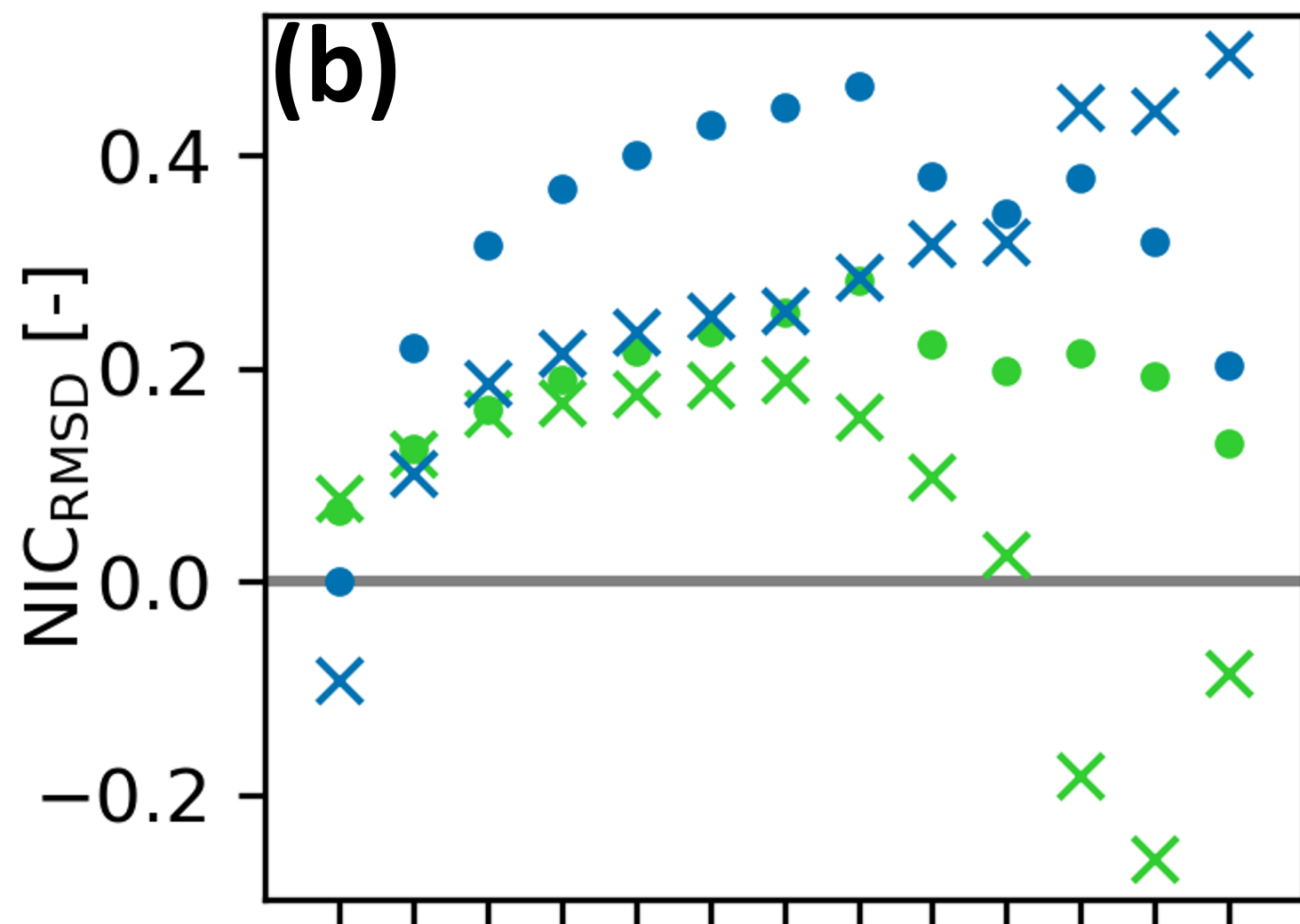
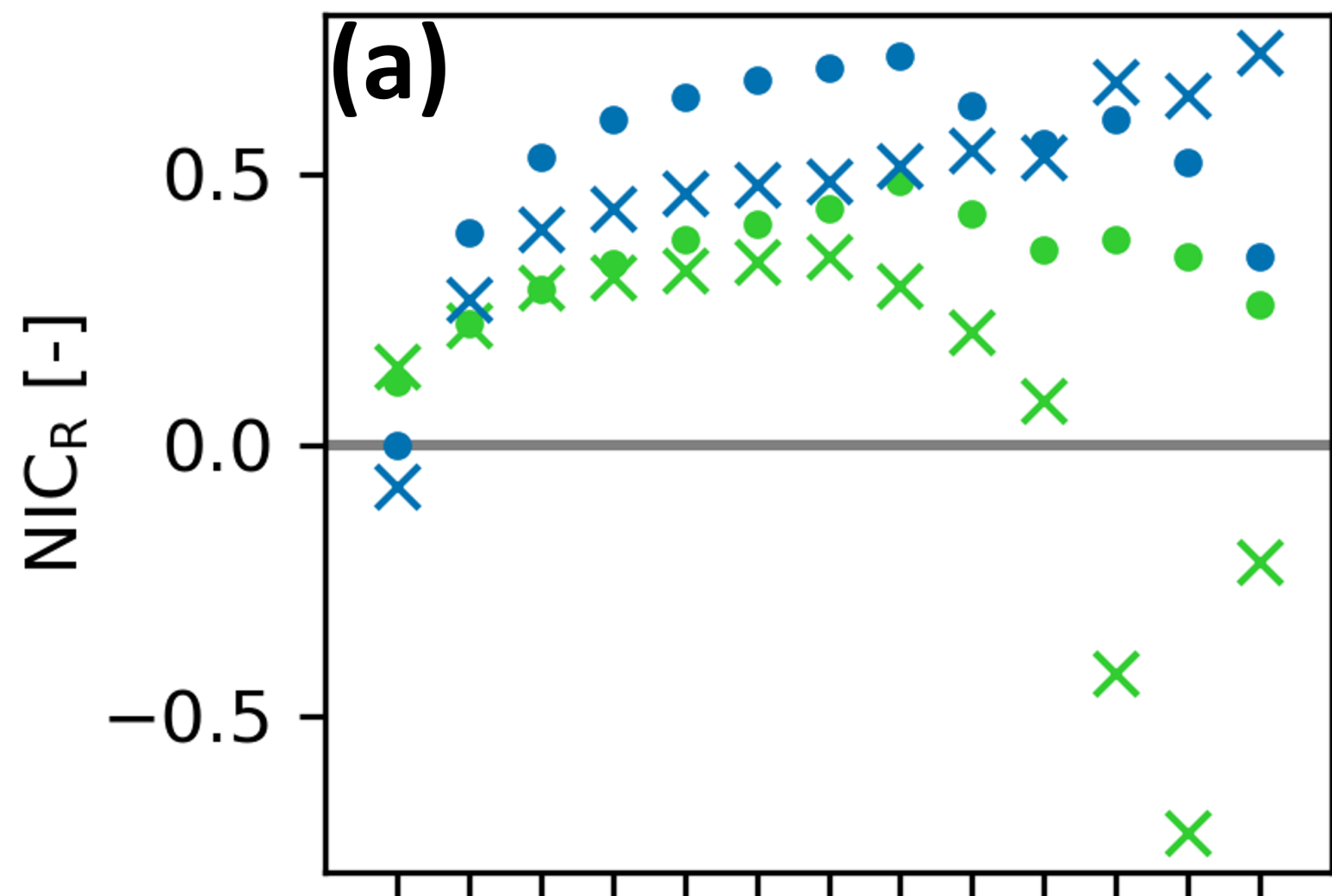


Figure 5.

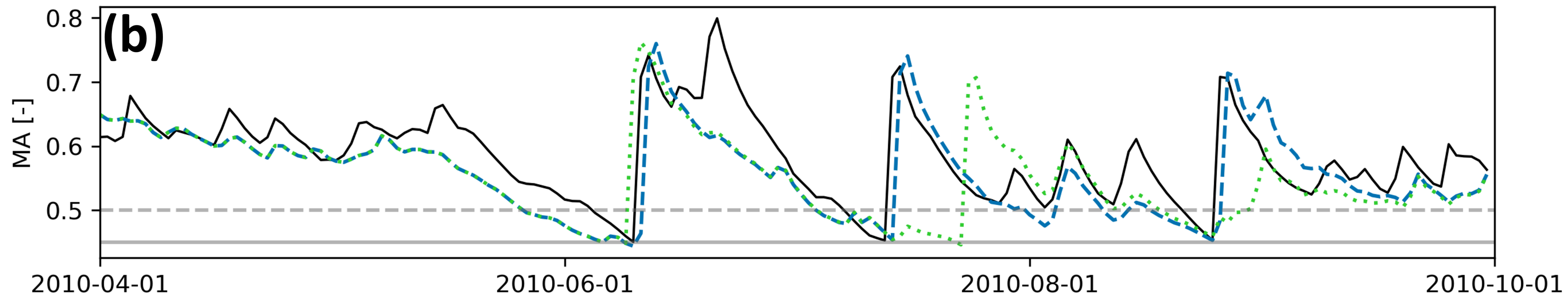
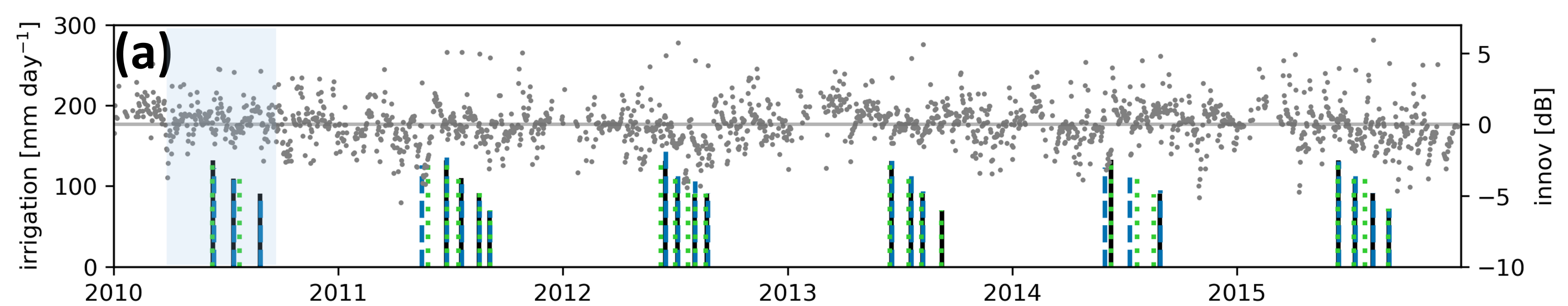


Figure 6.

